

DyG-Mamba: Continuous State Space Modeling on Dynamic Graphs

Dongyuan Li
Tokyo Institute of
Technology
lidy@lr.pi.titech.ac.jp

Shiyin Tan
Tokyo Institute of
Technology
tanshiyin@lr.pi.titech.ac.jp

Ying Zhang
RIKEN AIP
ying.zhang@riken.jp

Ming Jin
Griffith University
mingjinedu@gmail.com

Shirui Pan
Griffith University
s.pan@griffith.edu.au

Mamabu Okumura
Tokyo Institute of
Technology
oku@pi.titech.ac.jp

Renhe Jiang*
The University of Tokyo
jiangrh@csis.u-tokyo.ac.jp

Abstract

Dynamic graph learning aims to uncover evolutionary laws in real-world systems, enabling accurate social recommendation (link prediction) or early detection of cancer cells (classification). Inspired by the success of state space models, *e.g.*, Mamba, for efficiently capturing long-term dependencies in language modeling, we propose DyG-Mamba, a new continuous state space model (SSM) for dynamic graph learning. Specifically, we first found that using inputs as control signals for SSM is not suitable for continuous-time dynamic network data with irregular sampling intervals, resulting in models being insensitive to time information and lacking generalization properties. Drawing inspiration from the Ebbinghaus forgetting curve, which suggests that memory of past events is strongly correlated with time intervals rather than specific details of the events themselves, we directly utilize irregular time spans as control signals for SSM to achieve significant robustness and generalization. Through exhaustive experiments on 12 datasets for dynamic link prediction and dynamic node classification tasks, we found that DyG-Mamba achieves state-of-the-art performance on most of the datasets, while also demonstrating significantly improved computation and memory efficiency.

Keywords

Continuous-Time Dynamic Graphs, Temporal Link Prediction.

ACM Reference Format:

Dongyuan Li, Shiyin Tan, Ying Zhang, Ming Jin, Shirui Pan, Mamabu Okumura, and Renhe Jiang. 2018. DyG-Mamba: Continuous State Space Modeling on Dynamic Graphs. In *Proceedings of Make sure to enter the correct conference title from your rights confirmation email (Conference acronym 'XX)*. ACM, New York, NY, USA, 24 pages. <https://doi.org/XXXXXXX.XXXXXXX>

*Corresponding author.

Permission to make digital or hard copies of all or part of this work for personal or classroom use is granted without fee provided that copies are not made or distributed for profit or commercial advantage and that copies bear this notice and the full citation on the first page. Copyrights for components of this work owned by others than the author(s) must be honored. Abstracting with credit is permitted. To copy otherwise, or republish, to post on servers or to redistribute to lists, requires prior specific permission and/or a fee. Request permissions from permissions@acm.org.
Conference acronym 'XX, June 03–05, 2018, Woodstock, NY

© 2018 Copyright held by the owner/author(s). Publication rights licensed to ACM.
ACM ISBN 978-1-4503-XXXX-X/18/06
<https://doi.org/XXXXXXX.XXXXXXX>

1 Introduction

Dynamic graph learning aims to understand the node and link evolution laws behind many complex systems, *e.g.*, recommender systems [62, 65], traffic systems [2, 15], and social networks [1, 27, 49]. Despite the great success of current methods, there is still a core limitation: *existing methods lack the ability to efficiently and effectively track long-term temporal dependencies*. Specifically, RNN-based methods, *e.g.*, JODIE [27] and TGN [44], recurrently update the representation of current nodes by incorporating historical information. Although they efficiently capture long-term temporal dependencies, they suffer from vanishing/exploding gradients, leading to unsatisfactory performance. In contrast, Transformer-based models, *e.g.*, SimpleDyG [59] and DyGFormer [63], can effectively capture long-term dependencies but struggle with expensive computation costs, *i.e.*, the complexity of the self-attention mechanism grows quadratically as the size of input increases. Although many efforts have been dedicated to enhancing the efficiency of self-attention, *e.g.*, patching [22] or convolution [63], these methods inevitably make trade-offs between effectiveness and efficiency, thereby limiting their capability to establish long-term dependencies. Other methods using multi-layer perceptrons (MLPs) or graph neural networks (GNNs), *e.g.*, GraphMixer [6], FreeDyG [51], and TGAT [58], focus on short-term dependencies, and their performance often decreases as the sequence length increases [4, 6].

State space models (SSMs) seem to be a suitable framework to solve this problem, as they have shown great potential for long-term sequential modeling with linear time complexity [14, 16]. In particular, compared to previous SSMs like Hippo [11] and S4 [13], Mamba [10] sets parameters as input data-dependent variables to selectively copy previous hidden states, achieving better performance than Transformers in various tasks [41, 50, 66]. However, when vanilla Mamba is applied for dynamic graph learning, Figure 1(a) shows that Mamba significantly underperforms the Transformer-based DyGFormer. We explore three main reasons that hindered the application of Mamba to dynamic graphs. *Firstly, Mamba lacks sufficient utilization of time information with irregular time intervals*. The occurrence of events in dynamic graphs often follows different periodic patterns, resulting in irregular interaction timestamps. Effectively uncovering the underlying regularities in irregular temporal data can enhance dynamic graph learning capabilities [23]. However, as shown in Figure 1(b-d), when the time information is

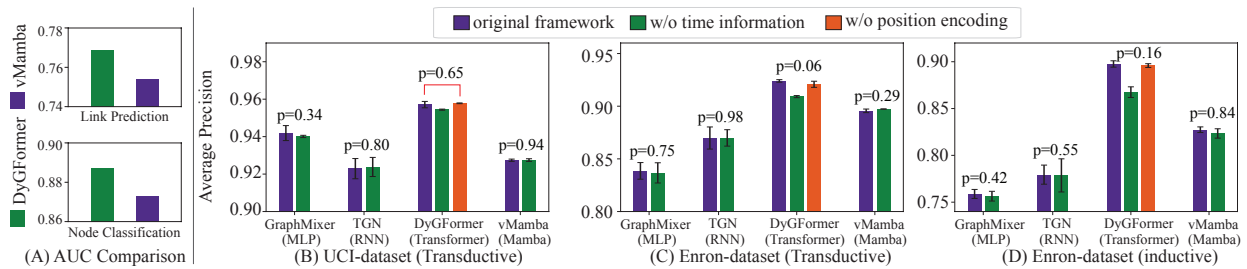


Figure 1: Experimental results for models with and w/o time information, and also for DyGFormer with positional encoding. $p = *$ indicates the p-value in the Student’s t-test [37]. vMamba represents the vanilla Mamba.

removed, only the Transformer-based DyGFormer shows a performance drop in most cases. It indicates that most previous studies including Mamba lack the ability to leverage irregular temporal information [23]. To further explore what DyGFormer learns from irregular time intervals, we simply replace time encoding with positional encoding [54], *i.e.*, replaces irregular time-spans as regular. We found that DyG-Mamba shows a slight performance drop. This indicates that it uses limited irregular time information to indicate sequence order. *Secondly, Mamba’s data-dependent selection leads to poor generalization for unseen nodes in inductive settings.* As shown in Figure 1(c-d), compared to DyGFormer, we observed that Mamba has a more obvious performance degradation in inductive settings than in transductive settings. Because Mamba set core parameters related to input data for selective copy, which limits its ability to effectively predict interactions between nodes that are unseen during the training process. *Thirdly, Mamba cannot support interactions between two input sequences.* For dynamic graph learning, many tasks require considering the semantic relatedness between two temporal neighborhoods (*i.e.*, history behaviors), which may also be a causal factor for the target interaction [56]. For example, in a temporal friendship network, if A and B are both friends with C, this can prompt a potential new friendship between A and B. Therefore, modeling mutual influences between two temporal neighborhoods can help in creating informative dynamic representations.

To address these issues, we propose DyG-Mamba, a new architecture for dynamic graph learning. Firstly, drawing inspiration from the Ebbinghaus Forgetting Curve theory [7], which suggests that “*human beings adhere to the same forgetting pattern for most things, which is strongly correlated with time rather than the content*”, we directly change the data-dependent parameter to a learnable time-spans-dependent parameter that automatically learn historical events’ periodicity with irregular time intervals and balance the aggregation between historical state and current input. Secondly, we theoretically and empirically demonstrate that among Mamba’s three data-dependent input parameters, the step size parameter Δ is the primary cause of its poor generalization. This parameter needs to be replaced with one that is time-span dependent. The other two parameters, B and C , are crucial for assessing the significance of historical states and should remain data-dependent. Finally, to enhance dynamic link prediction without adding extra computational overhead, we designed a linear cross-attention layer on top of the DyG-Mamba layer. This addition improves the model’s performance by better supporting the interaction of nodes in historical event sequences. The contributions are summarized as follows:

- To the best of our knowledge, we are the first to introduce SSMS for dynamic graph learning, achieving high efficiency and effectiveness in handling long-term temporal dependencies.
- We theoretically and empirically analyze the role of three core parameters of Mamba and replace one data-dependent parameter Δ with a learnable time-span-dependent parameter to better utilize irregular time information and enhances model’s generalization.
- We design a linear cross-attention architecture for DyG-Mamba to facilitate interaction between two historical event sequences, improving effectiveness without sacrificing efficiency.
- Extensive experimental results over 12 open datasets, including dynamic link prediction and node classification tasks, show that DyG-Mamba achieves SOTA performance with superior generalization and robustness. DyG-Mamba achieves higher precision with linear time and memory complexity than DyGFormer.

2 Related Work

Representation learning on dynamic graphs has recently attracted great attention [8, 20, 30, 31]. *Discrete-time methods* manually divide the dynamic graph into a sequence of snapshots with different resolutions (one day/an hour) and then combine GNNs (snapshot encoder) with recurrent models (dynamic tracker) to learn the representation of nodes [5, 40, 45, 46, 56, 61]. Their main common drawback is the necessity to predetermine the time granularity to create snapshots, ignoring the fine-grained temporal order of nodes/edges within each snapshot [58, 63]. In contrast, *continuous-time methods* directly use timestamps for representation learning. Based on the neural architectures, they can be classified into four classes, including *RNN-based methods*, *e.g.*, JODIE and TGN, *GNN-based methods*, *e.g.*, TGAT and DySAT [45], *MLP-based methods*, *e.g.*, GraphMixer and FreeDyG [51], and *Transformer-based methods*, *e.g.*, SimpleDyG [59] and DyGFormer. Additional techniques, such as ordinary differential equations [32, 33], random walks [23, 58], and temporal point process [19, 21], are also incorporated to learn continuous temporal information. Table 1 provides a detailed comparison between our method and the SOTAs including JODIE [27], DyRep [53], TGN [44], TGAT [58], CAWN [58], EdgeBank [43], TCL [56], GraphMixer [6], and DyGFormer [63], from the following angles: if the method could effectively handle unseen nodes during training (*i.e.*, inductive), capture long-term dependencies with both time and memory efficiency, exhibit robustness against noise, and effectively leverage irregular time-span information. We provide more related works and discussion in Appendix A.

Table 1: Comparison of Dynamic Graph Baselines. With a batch size of 200 and a sequence length of 512, a model is considered time and memory efficient if the running time and memory usage are less than GraphMixer, i.e., running time 250 seconds and memory usage 30,000 MB. Adding 50% noisy temporal edges, a performance drop of less than 10% indicates robustness.

	JODIE	DyRep	TGN	TGAT	CAWN	EdgeBank	TCL	GraphMixer	DyGFormer	DyG-Mamba
Inductive	✓	✓	✓	✓	✓	✗	✓	✓	✓	✓
Long-Term Dependency Capability	✗	✗	✗	✗	✗	✗	✗	✗	✓	✓
Time Efficient	✓	✗	✗	✗	✗	✓	✓	✓	✗	✓
Memory Efficient	✓	✗	✗	✗	✗	✓	✗	✓	✗	✓
Noise Robust	✗	✗	✓	✗	✗	✓	✗	✗	✓	✓
Irregular Time-Span Supportive	✗	✗	✗	✗	✗	✗	✗	✗	✗	✓

3 Preliminary

Dynamic Graph Learning. *Dynamic graphs* can be modeled as a sequence of non-decreasing chronological interactions $\mathcal{G} = \{(u_1, v_1, t_1), \dots, (u_\tau, v_\tau, t_\tau)\}$ with $0 \leq t_1 \leq \dots \leq \tau$, where $u_i, v_i \in \mathcal{V}$ denote the source and destination nodes of the i -th link and \mathcal{V} denote all nodes. Each node is associated with a node feature $\mathbf{x} \in \mathbb{R}^{d_V}$ and each interaction has a link feature $\mathbf{e}^t \in \mathbb{R}^{d_E}$, where d_V and d_E denote the dimensions of the node and the link features. Given the source node u , destination node v , timestamp t , and historical interactions before t , i.e., $\{(u', v', t') | t' < t\}$, *dynamic graph learning* aims to learn time-aware representations \mathbf{h}_u^t and \mathbf{h}_v^t for nodes u and v . We validate the learned representations via two common tasks: (i) *dynamic link prediction*, which predicts whether u and v are connected at t ; and (ii) *dynamic node classification*, which infers the class of u and v at t .

State Space Models. SSMs [10, 34, 41] define a linear mapping from input $\mathbf{u}(t) \in \mathbb{R}^d$ to output $\mathbf{y}(t) \in \mathbb{R}^d$ through a state-variable $\mathbf{h}(t) \in \mathbb{R}^{m \times d}$, formulated by:

$$\mathbf{h}'(t) = \mathbf{A}\mathbf{h}(t) + \mathbf{B}\mathbf{u}(t), \quad \mathbf{y}(t) = \mathbf{C}\mathbf{h}(t) + \mathbf{D}\mathbf{u}(t), \quad (1)$$

where $\mathbf{A} \in \mathbb{R}^{m \times m}$, $\mathbf{B}, \mathbf{C} \in \mathbb{R}^m$ are the weighting trainable parameters, and \mathbf{D} always equals to 0. For application to a discrete input sequence $(\mathbf{u}_1, \mathbf{u}_2, \dots, \mathbf{u}_\tau)$ instead of a continuous function, Eq.(1) can be discretized with a step size Δ , indicating the input’s resolution. Following [10], we consider to discretize SSMs using the zero-order hold (ZOH) discretization rule, which is formulated by:

$$\mathbf{h}_t = \bar{\mathbf{A}}\mathbf{h}_{t-1} + \bar{\mathbf{B}}\mathbf{u}_t, \quad \mathbf{y}_t = \mathbf{C}\mathbf{h}_t, \quad (2)$$

$$\text{where } \bar{\mathbf{A}} = \exp(\Delta\mathbf{A}), \quad \bar{\mathbf{B}} = (\Delta\mathbf{A})^{-1}(\exp(\Delta\mathbf{A}) - \mathbf{I})(\Delta\mathbf{B}).$$

By transforming the parameters from $(\Delta, \mathbf{A}, \mathbf{B})$ to $(\bar{\mathbf{A}}, \bar{\mathbf{B}})$, the SSM model becomes a sequence-to-sequence mapping framework from discrete input $\{\mathbf{u}_1, \mathbf{u}_2, \dots, \mathbf{u}_\tau\}$ to output $\{\mathbf{y}_1, \mathbf{y}_2, \dots, \mathbf{y}_\tau\}$.

4 Methodology

The overview of DyG-Mamba is shown in Figure 2(a), with two DyG-Mamba frameworks for dynamic link prediction in Figure 2(b) and node classification in Figure 2(c). To help readers better understand, we take the dynamic link prediction task as an instantiation. Specifically, to predict the interaction between nodes u and v at timestamp τ , we first extract first-hop interaction sequences of nodes u and v before τ . Next, in addition to computing the encoding of nodes, links, time, and co-neighbor frequencies, we also compute the encoding of normalized time-spans between any two continuous timestamps as control signals for the continuous SSM. Finally,

the outputs are averaged to derive representations of u and v at timestamp τ (i.e., \mathbf{h}_u^τ and \mathbf{h}_v^τ) for the dynamic link prediction.

4.1 Continuous-Time Dynamic Graph Encoding

Node, Edge, and Time Encodings. Most previous methods require nodes’ historical interactions from multiple hops for dynamic graph learning [44, 53]. Unlike them, we learn only from the nodes’ historical first-hop interactions, turning dynamic graph learning into simpler sequence learning problems. Specifically, the first-hop interaction sequence of length n for node u before time τ is defined as $S_u^\tau = \{(u, k_1, t_1), \dots, (u, k_n, t_n) | t_n < \tau\}$. Then, the encoding of S_u^τ includes node encodings $\mathbf{X}_{u,V}^\tau = \{\mathbf{v}_{k_1}, \dots, \mathbf{v}_{k_n}\} \in \mathbb{R}^{n \times d_V}$, edge encodings $\mathbf{X}_{u,E}^\tau = \{\mathbf{e}_{k_1}, \dots, \mathbf{e}_{k_n}\} \in \mathbb{R}^{n \times d_E}$, and time encodings $\mathbf{X}_{u,T}^\tau = \{\mathbf{t}_1, \dots, \mathbf{t}_n\} \in \mathbb{R}^{n \times d_T}$, where d_* ($* \in \{E, V, T\}$) are the dimensions of the encodings. In practice, the node/edge encodings are provided by the datasets. For the time encodings, we use angular frequency features $\boldsymbol{\omega} = \{\alpha^{-(i-1)/\beta}\}_{i=1}^{d_T}$ to encode the relative time intervals $\Delta t_j = \tau - t_j$ by the encoding function $\cos(\boldsymbol{\omega}\Delta t_j)$ into a d_T -dimensional vector. α and β are parameters that make $\Delta t_{\max} \times \alpha^{-(i-1)/\beta} \rightarrow 0$ when $i \rightarrow d_T$, and the cosine function helps project $\boldsymbol{\omega}\Delta t$ into $[-1, +1]$. Following [6], $\boldsymbol{\omega}$ remains constant during training to facilitate easier model optimization.

Co-occurrence Frequency Encodings. To consider the potential semantic relatedness between nodes’ historical interactions, we employ co-occurrence frequency encodings, following [63]. Formally, let the historical interactions of u and v be $\{a, b, v\}$ and $\{b, b, c, a\}$. The frequency of a, b, c , and v in two sequences is $[1, 1], [1, 2], [0, 1]$, and $[1, 0]$, respectively. The co-occurrence features of u and v could be denoted by $\mathbf{C}_u^\tau = [[1, 1], [1, 2], [1, 0]]^\top$ and $\mathbf{C}_v^\tau = [[1, 2], [1, 2], [0, 1], [1, 1]]^\top$. Then, we apply a function $f(\cdot) : \mathbb{R}^1 \rightarrow \mathbb{R}^{d_C}$ to encode the co-occurrence features by:

$$\mathbf{X}_{*,C}^\tau = (f(\mathbf{C}_*^\tau[:, 0]) + f(\mathbf{C}_*^\tau[:, 1]))\mathbf{W}_C + \mathbf{b}_C, \quad (3)$$

where $\mathbf{X}_{*,C}^\tau \in \mathbb{R}^{n \times d_C}$, $* \in \{u, v\}$ d_C is the dimension of the co-occurrence encoding, and \mathbf{W}_C and \mathbf{b}_C are trainable parameters. We implement $f(\cdot)$ by two-layer perception with ReLU activation [38].

Encoding Alignment. We align the encodings to the same dimension d with trainable weight $\mathbf{W}_* \in \mathbb{R}^{d_* \times d}$ and $\mathbf{b}_* \in \mathbb{R}^d$ to obtain $\mathbf{Z}_{u,*}^\tau \in \mathbb{R}^{n \times d}$, formulated by:

$$\mathbf{Z}_{u,*}^\tau = \mathbf{X}_{u,*}^\tau \mathbf{W}_* + \mathbf{b}_*, \quad \text{where } * \in \{N, E, T, C\}. \quad (4)$$

Finally, we concatenate $\mathbf{Z}_u^\tau = \mathbf{Z}_{u,V}^\tau \parallel \mathbf{Z}_{u,E}^\tau \parallel \mathbf{Z}_{u,T}^\tau \parallel \mathbf{Z}_{u,C}^\tau$ as the aligned embedding for u with $\mathbf{Z}_u^\tau \in \mathbb{R}^{L_u \times 4d}$.

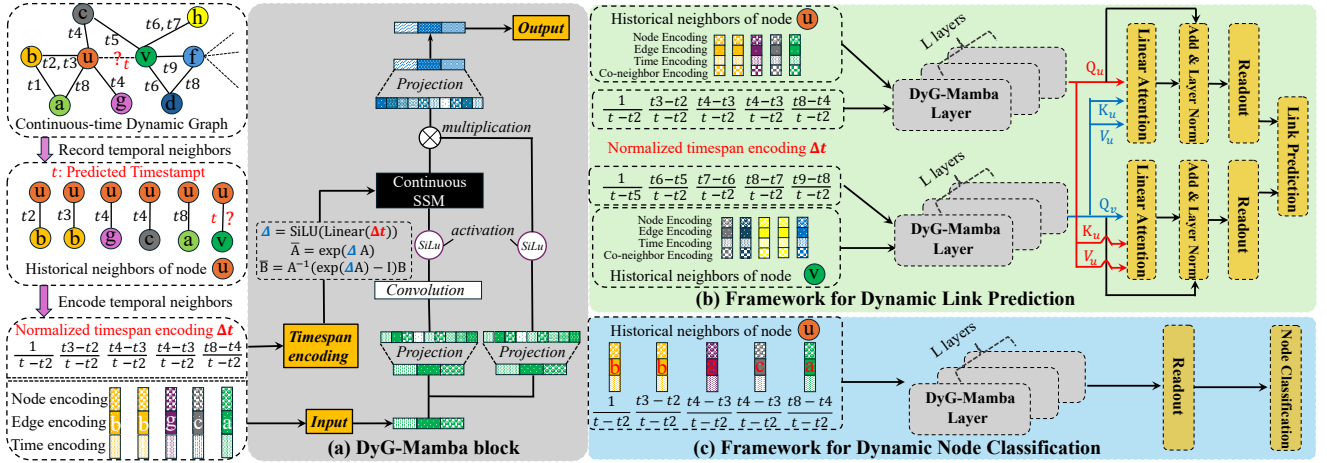


Figure 2: Overview of the DyG-Mamba (a) and its frameworks for downstream tasks (b, c). Pseudocodes are in Appendix H.

4.2 SSMs for Dynamic Graph Modeling

In Eq.(2), DyG-Mamba has three core parameters: Δ , B , and C . Specifically, Δ determines how much historical memory is forgotten, and B and C measure the similarity between previous inputs and the target output. In this section, we theoretically analysis their roles. We first introduce the definition of the parameter Δ in Theorem 1.

THEOREM 1. For a general formulation of the linear time-invariant ODE of the form $\frac{d}{dt}\mathbf{h}(t) = \mathbf{A}\mathbf{h}(t) + \mathbf{B}\mathbf{u}(t)$ for some input function $\mathbf{u}(t)$, the general method for discretizing the ODE with each step size Δt , can be calculated in closed-form between t and $t+\Delta t$ as $\mathbf{h}(t + \Delta t) = e^{\Delta t \mathbf{A}}\mathbf{h}(t) + \left(\int_{s=0}^{\Delta t} e^{s\mathbf{A}} ds\right)\mathbf{B}\mathbf{u}(t)$ if the control input $\mathbf{u}(t)$ remains constant between t and $t+\Delta t$. If \mathbf{A} is invertible, $\mathbf{h}(t + \Delta t) = e^{\Delta t \mathbf{A}}\mathbf{h}(t) + (\Delta t \mathbf{A})^{-1}(e^{\Delta t \mathbf{A}} - \mathbf{I})(\Delta t \mathbf{B})\mathbf{u}(t)$.

Mamba [10] focuses on language sequences, which assumes that successive word pairs have the same interval, e.g., $\Delta t = 1$ in Theorem 1. To selectively copy some previous inputs, Mamba takes the current input $\mathbf{u}(t)$ as control signals to replace the previous fixed Δt with $\Delta t = \text{SiLU}(\text{Linear}(\mathbf{u}(t)))$, where SiLU is an activation function. However, when applied to dynamic graphs, Mamba cannot effectively use irregular time information (Figure 1), and its data-dependent strategy leads to poor performance in inductive scenarios (w/o Time-Span vs. DyG-Mamba in Figure 5). The Ebbinghaus Forgetting Curve theory [7] suggests that historical memory is strongly correlated with time-spans between events rather than events themselves. Considering dynamic graphs naturally have irregular time intervals, we can use time-spans between any two timestamps t_{i-1} and t_i as control signals, formulated by:

$$\Delta t_i = \text{SiLU}(\text{Linear}(\cos(\omega(t_{i+1} - t_i) / (\tau - t_1))))), \quad (5)$$

where Linear represents linear layers and we set $\Delta t_1 = 1/(\tau - t_1)$. We then take Z_u^t as input for DyG-Mamba and the time-span sequence $\{\Delta t_i\}_{i=1}^n$ as control signals for continuous SSMs. Z_u^t first passes through a linear layer followed by a 1D convolution layer and SiLU activation function, which can be formulated by

$$M_u^t = \text{SiLU}(\text{Conv1D}(\text{Linear}(Z_u^t))). \quad (6)$$

Then, we initialize \mathbf{A} as a dialogue matrix based on [16] and set $\{\Delta t_i\}_{i=1}^n$ according to Eq.(5). We define $\mathbf{B} = \text{Linear}_B(M_u^t)$ and $\mathbf{C} = \text{Linear}_C(M_u^t)$. M_u^t can pass through the continuous SSM layer to learn new representations, which could be formulated by:

$$\widehat{Z}_u^t = \text{SSM}(M_u^t, \mathbf{B}, \mathbf{C}, \{\Delta t_i\}_{i=1}^n), \quad (7)$$

where the k -th generated output of \widehat{Z}_u^t could be formulated by:

$$\mathbf{h}_k = \overline{\mathbf{A}}_k \mathbf{h}_{k-1} + \overline{\mathbf{B}}_k \mathbf{u}_k, \quad \widehat{z}_k^t = \overline{\mathbf{C}}_k \mathbf{h}_k, \quad (8)$$

where $\overline{\mathbf{A}}_k = \exp(\Delta t_k \mathbf{A})$, $\overline{\mathbf{B}}_k = (\Delta t_k \mathbf{A})^{-1}(\exp(\Delta t_k \mathbf{A}) - \mathbf{I})(\Delta t_k \mathbf{B})$ and $\overline{\mathbf{C}}_k = \mathbf{C}_k$. To theoretically demonstrate that time-span encoding can control the importance between historical memory and current input, we first give the following Theorem 2.

THEOREM 2. Let \mathbf{A} be diagonalizable as $\mathbf{A} = \mathbf{V}\mathbf{\Lambda}\mathbf{V}^{-1}$ with eigenvalues $\{\lambda_1, \dots, \lambda_N\}$. Given Δt_k , $\overline{\mathbf{A}}_k = \text{diag}(e^{\lambda_1 \Delta t_k}, \dots, e^{\lambda_N \Delta t_k})$ and $\overline{\mathbf{B}}_k = (\lambda_1^{-1}(e^{\lambda_1 \Delta t_k} - 1), \dots, \lambda_N^{-1}(e^{\lambda_N \Delta t_k} - 1))$, the i -th coordinate of \mathbf{h}_k in Eq.(8) can be denoted as $h_{i,k} = e^{\lambda_i \Delta t_k} h_{i,k-1} + \lambda_i^{-1}(e^{\lambda_i \Delta t_k} - 1)u_{i,k}$.

Following [16], the real part of the elements of λ_i is restricted to be negative. According to Theorem 2, if Δt_k is small enough, we obtain $|\lambda_i| \Delta t_k \approx 0$, i.e., $h_{i,k} \approx h_{i,k-1}$, demonstrating that a small time-span Δt_k persists the historical state and ignores the current input. And a larger Δt_k makes $\lambda_i \Delta t_k \ll 0$ and $h_{i,k} \approx -\lambda_i^{-1} u_k$, i.e., the information from the previous timesteps would be forgotten, similar to a ‘‘forget’’ gate in LSTM [18].

We then show how the parameters \mathbf{B} and \mathbf{C} selectively copy previous inputs according to Theorem 3.

THEOREM 3. Parameters \mathbf{B} and \mathbf{C} can help selectively copy the previous input through the causal attention mechanism. Considering \mathbf{u}_k as k -th column of M_u^t , Eq.(8) can be further decomposed as follows:

$$\begin{aligned} \widehat{z}_k^t &= \overline{\mathbf{C}}_k \left[\prod_{i=0}^{k-2} \overline{\mathbf{A}}_{k-i} \overline{\mathbf{B}}_i \mathbf{u}_1 + \dots + \overline{\mathbf{C}}_k \left[\prod_{i=0}^{k-j} \overline{\mathbf{A}}_{k-i} \overline{\mathbf{B}}_{j-1} \mathbf{u}_{j-1} + \dots + \overline{\mathbf{C}}_k \overline{\mathbf{B}}_k \mathbf{u}_k \right] \right] \\ &= e^{(\sum_{i=0}^{k-2} \Delta t_{k-i} \mathbf{A})} \overline{\mathbf{C}}_k \overline{\mathbf{B}}_1 \mathbf{u}_1 + \dots + e^{(\sum_{i=0}^{k-j-1} \Delta t_{k-i} \mathbf{A})} \overline{\mathbf{C}}_k \overline{\mathbf{B}}_j \mathbf{u}_j + \dots + \overline{\mathbf{C}}_k \overline{\mathbf{B}}_k \mathbf{u}_k, \end{aligned}$$

where $\overline{\mathbf{C}}_k$ can be considered as the query of k -th input \mathbf{u}_k and $\overline{\mathbf{B}}_j$ can be considered as key of \mathbf{u}_j . Thus, $\overline{\mathbf{C}}_k \overline{\mathbf{B}}_j$ can measure the similarity.

Table 2: AP for inductive dynamic link prediction with random negative sampling strategies. The best and second-best results are emphasized by bold and underlined fonts. Please note that N/A means Not Applicable.

Datasets	JODIE	DyRep	TGAT	TGN	CAWN	EdgeBank	TCL	GraphMixer	DyGFormer	DyG-Mamba
Wikipedia	94.82±0.20	92.43±0.37	96.22±0.07	97.83±0.04	98.24±0.03	N/A	96.22±0.17	96.65±0.02	<u>98.59±0.03</u>	98.65±0.03
Reddit	96.50±0.13	96.09±0.11	97.09±0.04	97.50±0.07	98.62±0.01	N/A	94.09±0.07	95.26±0.02	<u>98.84±0.02</u>	98.88±0.00
MOOC	79.63±1.92	81.07±0.44	85.50±0.19	<u>89.04±1.17</u>	81.42±0.24	N/A	80.60±0.22	81.41±0.21	86.96±0.43	90.20±0.06
LastFM	81.61±3.82	83.02±1.48	78.63±0.31	81.45±4.29	89.42±0.07	N/A	73.53±1.66	82.11±0.42	<u>94.23±0.09</u>	95.13±0.08
Enron	80.72±1.39	74.55±3.95	67.05±1.51	77.94±1.02	86.35±0.51	N/A	76.14±0.79	75.88±0.48	<u>89.76±0.34</u>	91.14±0.07
Social Evo.	91.96±0.48	90.04±0.47	91.41±0.16	90.77±0.86	79.94±0.18	N/A	91.55±0.09	91.86±0.06	<u>93.14±0.04</u>	93.23±0.01
UCI	79.86±1.48	57.48±1.87	79.54±0.48	88.12±2.05	92.73±0.06	N/A	87.36±2.03	91.19±0.42	<u>94.54±0.12</u>	<u>94.15±0.04</u>
Can. Parl.	53.92±0.94	54.02±0.76	55.18±0.79	54.10±0.93	55.80±0.69	N/A	54.30±0.66	55.91±0.82	<u>87.74±0.71</u>	90.05±0.86
US Legis.	54.93±2.29	57.28±0.71	51.00±3.11	<u>58.63±0.37</u>	53.17±1.20	N/A	52.59±0.97	50.71±0.76	54.28±2.87	59.52±0.54
UN Trade	59.65±0.77	57.02±0.69	61.03±0.18	58.31±3.15	<u>65.24±0.21</u>	N/A	62.21±0.12	62.17±0.31	64.55±0.62	65.87±0.40
UN Vote	56.64±0.96	54.62±2.22	52.24±1.46	<u>58.85±2.51</u>	49.94±0.45	N/A	51.60±0.97	50.68±0.44	55.93±0.39	59.89±1.04
Contact	94.34±1.45	92.18±0.41	95.87±0.11	93.82±0.99	89.55±0.30	N/A	91.11±0.12	90.59±0.05	<u>98.03±0.02</u>	98.12±0.04
Avg. Rank	5.83	6.91	6.20	4.83	4.91	N/A	6.70	6.00	<u>2.50</u>	1.08

Finally, after SSM layer, the output can be formulated by:

$$\mathbf{Z}_{u,out}^r = (\widehat{\mathbf{Z}}_u^r \odot \text{SiLU}(\text{Linear}(\mathbf{Z}_u^r)))\mathbf{W}_{out} + \mathbf{b}_{out}, \quad (9)$$

where \odot is element-wise dot product, and \mathbf{W}_{out} and \mathbf{b}_{out} are trainable parameters. We proof all theorems in Appendix B.

4.3 DyG-Mamba for Downstream Tasks

Temporal Link Prediction. In Figure 2(b), we employ a two-stream DyG-Mamba encoder to individually deal with each sequence. Inspired by linear attention [25], which reduces time and memory complexity, we then interact the two streams at the semantic level through a linear cross-attention layer, formulated by:

$$\text{Linear Attention}(\mathbf{Q}, \mathbf{K}, \mathbf{V}) = \frac{\phi(\mathbf{Q}_i)^\top \sum_{j=1}^i \phi(\mathbf{K}_j) \mathbf{V}_j^\top}{\phi(\mathbf{Q}_i)^\top \sum_{j=1}^i \phi(\mathbf{K}_j)}, \quad (10)$$

$$\mathbf{Q}_*^r, \mathbf{K}_*^r, \mathbf{V}_*^r = \mathbf{Z}_{*,out}^r \mathbf{W}_Q, \mathbf{Z}_{*,out}^r \mathbf{W}_K, \mathbf{Z}_{*,out}^r \mathbf{W}_V, \quad * \in \{u, v\}, \quad (11)$$

$$\mathbf{O}_*^r = \text{Linear Attention}(\mathbf{Q}_*^r, \mathbf{K}_*^r, \mathbf{V}_*^r), \quad * \in \{u, v\}, \quad (12)$$

$$\mathbf{H}_*^r = \text{LayerNorm}(\text{Linear}(\mathbf{O}_*^r + \mathbf{Q}_*^r)), \quad * \in \{u, v\}, \quad (13)$$

where $\phi(x) = \text{elu}(x) + 1$ and $\text{elu}(\cdot)$ is an activation function [3]. The co-attention operation in Eq.(12) allows the encoder to emphasize relevant shared semantics and suppress irrelevant ones. We use readout function $\mathbb{R}^{L \times 4d} \rightarrow \mathbb{R}^{1 \times 4d}$, i.e., MEAN pooling, to obtain node embeddings $\mathbf{h}_*^r = \text{MEAN}(\mathbf{H}_*^r)$ with $* \in \{u, v\}$. Finally, we use an MLP to concatenate representations of two nodes as inputs and return the predicted probability \hat{y} as output, formulated by:

$$\hat{y} = \text{Softmax}(\text{Linear}(\text{RELU}(\text{Linear}(\mathbf{h}_u^r \parallel \mathbf{h}_v^r))). \quad (14)$$

We adopt binary cross-entropy loss for dynamic link prediction.

Temporal Node Classification. After obtaining sequential node representations $\mathbf{H}_{u,out}^r \in \mathbb{R}^{L \times 3d}$ without co-neighbor encoding, node embeddings are calculated by $\mathbf{h}_u^r = \text{MEAN}(\mathbf{H}_{u,out}^r)$, and we use the binary cross-entropy loss function for node classification.

Computational Efficiency. Assuming the batch size is b , the feature dimension is d , and the sequence length is L , the memory and time complexities of DyG-Mamba are $O(bLd)$. DyGFormer exhibits quadratic memory and time complexities as $O(bL^2d)$, showing the efficiency of DyG-Mamba. Refer to Appendix C for more details.

5 Experiments

Datasets and Baselines. We evaluate model’s performance on 12 datasets, ranging from social networks to transportation networks [43]. Details are listed in Appendix D.2. We split each dataset with the ratio of 70%/15%/15% for training/validation/testing. We select nine best-performing dynamic graph learning baselines, including RNN-based methods: JODIE, DyRep, TGN and CAWN, a GNN-based method: TGAT, a memory-based method: EdgeBank, a MLP-based method: GraphMixer, and Transformer-based methods: TCL and DyGFormer. Details are listed in Appendix A.3.

Evaluation Details and Metrics. For dynamic link prediction, following [43, 51, 63], we evaluate baselines with two settings: the *transductive setting* aims to predict future links between nodes observed during training, and the *inductive setting* predicts future links between unseen nodes. We use AP and AUC-ROC as the evaluation metrics. [43] found that random negative sampling may not provide a complete evaluation. Thus, following their studies, we adopt random (*rnd*), historical (*hist*), and inductive (*ind*) negative sampling for evaluation Appendix D. For dynamic node classification, we estimate the state of a node in a given interaction at a specific time and use AUC-ROC as the evaluation metric.

Implementation Details. For a fair comparison, we use DyGLib [63] that reproduce all baselines via the same training/inference pipeline. We use the Adam optimizer [26] with a learning rate of 0.0001. We train the models for 100 epochs and use the early stopping strategy with a patience of 20. We select the model that achieves the best performance in the validation set for testing. We run methods five times and report the average performance to eliminate deviations.

5.1 Quantitative Evaluation

Performance on Dynamic Node Classification. Table 3 shows the AUC-ROC results on dynamic node classification. DyG-Mamba achieves SOTA performance on the Reddit dataset and second-best performance on the Wikipedia dataset. In addition, DyG-Mamba achieves the best average rank of 1.5 compared to the second-best DyGFormer with 3.5 AUC-ROC results for all baselines in Table 3.

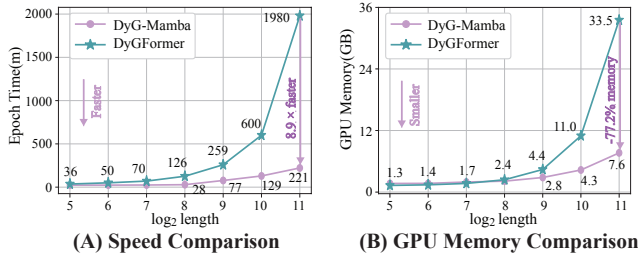
Performance on Dynamic Link Prediction. To demonstrate the effectiveness and generalizability of DyG-Mamba, we perform evaluations in two different experimental settings: transductive

Table 3: Performance on dynamic node classification.

Methods	Wikipedia	Reddit	Avg. Rank
JODIE	88.99±1.05	60.37±2.58	5.00
DyRep	86.39±0.98	63.72±1.32	6.00
TGAT	84.09±1.27	70.04±1.09	5.00
TGN	86.38±2.34	63.27±0.90	7.00
CAWN	84.88±1.33	66.34±1.78	6.00
EdgeBank	N/A	N/A	N/A
TCL	77.83±2.13	68.87±2.15	6.00
GraphMixer	86.80±0.79	64.22±3.32	5.00
DyGFormer	87.44±1.08	68.00±1.74	3.50
DyG-Mamba	88.58±0.92	70.79±1.97	1.50

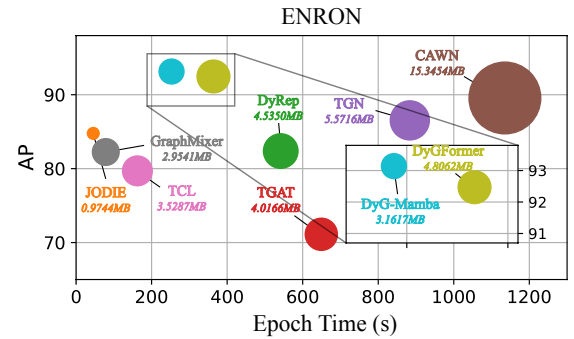
and inductive settings. Table 2 reports the results in the inductive setting with *rnd* negative sampling. Table 10 shows the results with *hist/ind* negative sampling. From these tables, we observe that DyG-Mamba achieves the best performance on 11 datasets and achieves a best average rank of 1.91/1.69 on AP/AUC across three negative sampling strategies, while the best-performing baseline DyGFormer achieves only 3.47/3.28. Table 4 shows the results in the transductive setting. Among ten models, DyG-Mamba achieves the best/second-best performance on 11, eight, and ten datasets in three negative sampling strategies, respectively. DyG-Mamba also achieves the best average rank of 1.94/2.05 on AP/AUC, while the best-performing baseline DyGFormer achieves only 3.16/3.30. Please refer to Appendix E.2 for the results of AUC-ROC. Furthermore, as Figure 6(A) shows DyG-Mamba outperforms DyGFormer in terms of averaged AUC scores, achieving improvements of 3.64% and 1.83% in dynamic link prediction and node classification tasks.

Comparison of Time and Memory. To demonstrate the efficiency of DyG-Mamba, we present a comprehensive comparison with the best-performing Transformer-based backbone, DyGFormer. As shown in Figures 3(A)-(B), DyG-Mamba requires significantly less training time and memory usage than DyGFormer when handling long sequences. *Specifically, DyG-Mamba is 8.9 times faster than DyGFormer and saves 77.2% GPU memory with a sequence length of 2,048.* For a fair comparison, we do not use the patching technique for both DyGFormer and DyG-Mamba.

**Figure 3: Comparison of DyGFormer and DyG-Mamba with varying lengths. (A) time and (B) memory consumption.**

Comparison of Training Time and Parameters. By setting the sequence length to 256, we conduct a comparative analysis of

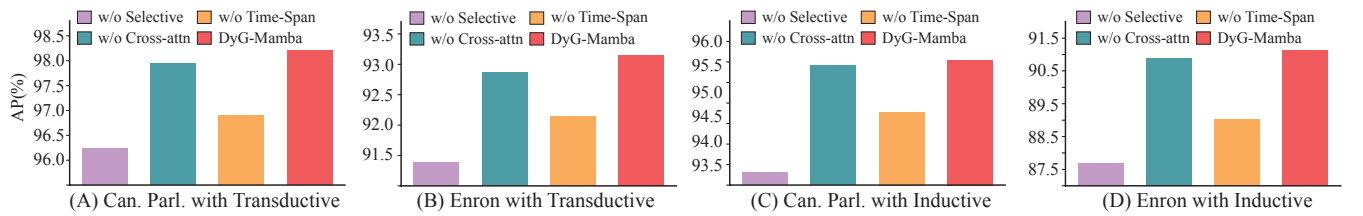
the performance, training time per epoch (measured in seconds), and size of trainable parameters (measured in Megabyte, *i.e.*, MB) between DyG-Mamba and all baselines on the Enron dataset, as shown in Figure 4, and other datasets, as shown in Figure 10. Obviously, CAWN requires the longest training time and a substantial number of parameters, because it conducts random walks on dynamic graphs to collect time-aware sequences for dynamic graph learning. On the other hand, simpler methods, *e.g.*, the MLP-based GraphMixer and the RNN-based JODIE, have fewer parameters, but exhibit a significant performance gap compared to the best-performing DyGFormer and DyG-Mamba. Overall, DyG-Mamba achieves the best performance with a small size of trainable parameters and a moderate training time required per epoch.

**Figure 4: Comparison of model performance (AP), parameter size (size of the circle) and training time (seconds) per epoch.**

Discussion and Analysis. From the above experimental results, we obtain the following three conclusions: (i) *Higher Effectiveness.* DyG-Mamba can achieve the best performance in temporal link prediction and node classification tasks, demonstrating that DyG-Mamba is more suitable for dealing with dynamic graph learning. The reason is that DyG-Mamba can better track long-term temporal dependencies, as detailed in Figure 7. Compared with the best-performing baseline DyGFormer, based on self-attention aggregation, DyG-Mamba based on the causal attention mechanism, which can capture the evolving nature of node representations and remove irrelevant historical neighbors for each timestamp (Figure 6). Finally, the cross-attention scheme also helps DyG-Mamba exploit the correlations between nodes, which are often predictive of future links (please refer to Figure 5). (ii) *Better Generalizability.* By incorporating time-spans as control signals for SSMs, DyG-Mamba can establish a strong correlation between time-spans and evolution laws of dynamic networks, *i.e.*, how to balance historical memory with the current input. In Figure 5, by removing time-span information, we observe a significant drop in the inductive setting. On the other hand, compared to data-independent Mamba, time information is one kind of anonymous information, and DyG-Mamba can improve generalization and easily apply to unseen nodes (w/o Time-Span vs. DyG-Mamba in Figure 5). (iii) *Greater Efficiency.* DyG-Mamba leverages the advantages of SSMs, employing a limited number of parameters to remember or forget historical information, thus achieving memory efficiency. Using parallel scanning and hardware-aware training strategies, the time complexity of DyG-Mamba approaches linearity (Figure 3).

Table 4: AP for transductive dynamic link prediction with random, historical, and inductive negative sampling strategies.

NSS	Datasets	JODIE	DyRep	TGAT	TGN	CAWN	EdgeBank	TCL	GraphMixer	DyGFormer	DyG-Mamba
rnd	Wikipedia	96.50 ± 0.14	94.86 ± 0.06	96.94 ± 0.06	98.45 ± 0.06	98.76 ± 0.03	90.37 ± 0.00	96.47 ± 0.16	97.25 ± 0.03	<u>99.03 ± 0.02</u>	<u>99.08 ± 0.09</u>
	Reddit	98.31 ± 0.14	98.22 ± 0.04	98.52 ± 0.02	98.63 ± 0.06	99.11 ± 0.01	94.86 ± 0.00	97.53 ± 0.02	97.31 ± 0.01	<u>99.22 ± 0.01</u>	<u>99.27 ± 0.00</u>
	MOOC	80.23 ± 2.44	81.97 ± 0.49	85.84 ± 0.15	<u>89.15 ± 1.60</u>	80.15 ± 0.25	57.97 ± 0.00	82.38 ± 0.24	82.78 ± 0.15	87.52 ± 0.49	<u>90.25 ± 0.09</u>
	LastFM	70.85 ± 2.13	71.92 ± 2.21	73.42 ± 0.21	77.07 ± 3.97	86.99 ± 0.06	79.29 ± 0.00	67.27 ± 2.16	75.61 ± 0.24	<u>93.00 ± 0.12</u>	<u>94.23 ± 0.01</u>
	Enron	84.77 ± 0.30	82.38 ± 3.36	71.12 ± 0.97	86.53 ± 1.11	89.56 ± 0.09	83.53 ± 0.00	79.70 ± 0.71	82.25 ± 0.16	<u>92.47 ± 0.12</u>	<u>93.14 ± 0.08</u>
	Social Evo.	89.89 ± 0.55	88.87 ± 0.30	93.16 ± 0.17	93.57 ± 0.17	84.96 ± 0.09	74.95 ± 0.00	93.13 ± 0.16	93.37 ± 0.07	<u>94.73 ± 0.01</u>	<u>94.77 ± 0.01</u>
	UCI	89.43 ± 1.09	65.14 ± 2.30	79.63 ± 0.70	92.34 ± 1.04	95.18 ± 0.06	76.20 ± 0.00	89.57 ± 1.63	93.25 ± 0.57	<u>95.79 ± 0.17</u>	<u>96.14 ± 0.14</u>
	Can. Parl.	69.26 ± 0.31	66.54 ± 2.76	70.73 ± 0.72	70.88 ± 2.34	69.82 ± 2.34	64.55 ± 0.00	68.67 ± 2.67	77.04 ± 0.46	<u>97.36 ± 0.45</u>	<u>98.20 ± 0.52</u>
	US Legis.	75.05 ± 1.52	<u>75.34 ± 0.39</u>	68.52 ± 3.16	<u>75.99 ± 0.58</u>	70.58 ± 0.48	58.39 ± 0.00	69.59 ± 0.48	70.74 ± 1.02	71.11 ± 0.59	73.66 ± 1.13
	UN Trade	64.94 ± 0.31	63.21 ± 0.93	61.47 ± 0.18	65.03 ± 1.37	65.39 ± 0.12	60.41 ± 0.00	62.21 ± 0.03	62.61 ± 0.27	<u>66.46 ± 1.29</u>	<u>68.51 ± 0.17</u>
	UN Vote	63.91 ± 0.81	62.81 ± 0.80	52.21 ± 0.98	<u>65.72 ± 2.17</u>	52.84 ± 0.10	58.49 ± 0.00	51.90 ± 0.30	52.11 ± 0.16	55.55 ± 0.42	<u>64.74 ± 1.48</u>
	Contact	95.31 ± 1.33	95.98 ± 0.15	96.28 ± 0.09	96.89 ± 0.56	90.26 ± 0.28	92.58 ± 0.00	92.44 ± 0.12	91.92 ± 0.03	<u>98.29 ± 0.01</u>	<u>98.38 ± 0.01</u>
	Avg. Rank	6.08	6.83	6.67	3.33	5.50	8.42	7.92	6.25	<u>2.67</u>	<u>1.33</u>
hist	Wikipedia	83.01 ± 0.66	79.93 ± 0.56	87.38 ± 0.22	86.86 ± 0.33	71.21 ± 1.67	73.35 ± 0.00	<u>89.05 ± 0.39</u>	<u>90.90 ± 0.10</u>	82.23 ± 2.54	82.35 ± 1.25
	Reddit	80.03 ± 0.36	79.83 ± 0.31	79.55 ± 0.20	<u>81.22 ± 0.61</u>	80.82 ± 0.45	73.59 ± 0.00	77.14 ± 0.16	78.44 ± 0.18	<u>81.57 ± 0.67</u>	81.02 ± 0.19
	MOOC	78.94 ± 1.25	75.60 ± 1.12	82.19 ± 0.62	<u>87.06 ± 1.93</u>	74.05 ± 0.95	60.71 ± 0.00	77.06 ± 0.41	77.77 ± 0.92	85.85 ± 0.66	<u>87.42 ± 1.57</u>
	LastFM	74.35 ± 3.81	74.92 ± 2.46	71.59 ± 0.24	76.87 ± 4.64	69.86 ± 0.43	73.03 ± 0.00	59.30 ± 2.31	72.47 ± 0.49	<u>81.57 ± 0.48</u>	<u>84.08 ± 0.45</u>
	Enron	69.85 ± 2.70	71.19 ± 2.76	64.07 ± 1.05	73.91 ± 1.76	64.73 ± 0.36	76.53 ± 0.00	70.66 ± 0.39	<u>77.98 ± 0.92</u>	75.63 ± 0.73	<u>77.85 ± 1.20</u>
	Social Evo.	87.44 ± 6.78	93.29 ± 0.43	95.01 ± 0.44	94.45 ± 0.56	85.53 ± 0.38	80.57 ± 0.00	94.74 ± 0.31	94.93 ± 0.31	<u>97.38 ± 0.14</u>	<u>97.35 ± 0.18</u>
	UCI	75.24 ± 5.80	55.10 ± 3.14	68.27 ± 1.37	80.43 ± 2.12	65.30 ± 0.43	65.50 ± 0.00	80.25 ± 2.74	<u>84.11 ± 1.35</u>	<u>82.17 ± 0.82</u>	81.36 ± 0.14
	Can. Parl.	51.79 ± 0.63	63.31 ± 1.23	67.13 ± 0.84	68.42 ± 3.07	66.53 ± 2.77	63.84 ± 0.00	65.93 ± 3.00	74.34 ± 0.87	<u>97.00 ± 0.31</u>	<u>97.39 ± 0.29</u>
	US Legis.	51.71 ± 5.76	<u>86.88 ± 2.25</u>	62.14 ± 6.60	74.00 ± 7.57	68.82 ± 8.23	63.22 ± 0.00	80.53 ± 3.95	81.65 ± 1.02	85.30 ± 3.88	<u>88.86 ± 1.40</u>
	UN Trade	61.39 ± 1.83	59.19 ± 1.07	55.74 ± 0.91	58.44 ± 5.51	55.71 ± 0.38	<u>81.32 ± 0.00</u>	55.90 ± 1.17	57.05 ± 1.22	64.41 ± 1.40	<u>65.11 ± 0.19</u>
	UN Vote	<u>70.02 ± 0.81</u>	69.30 ± 1.12	52.96 ± 2.14	69.37 ± 3.93	51.26 ± 0.04	<u>84.89 ± 0.00</u>	52.30 ± 2.35	51.20 ± 1.60	60.84 ± 1.58	61.17 ± 2.64
	Contact	95.31 ± 2.13	96.39 ± 0.20	96.05 ± 0.52	93.05 ± 2.35	84.16 ± 0.49	88.81 ± 0.00	93.86 ± 0.21	93.36 ± 0.41	<u>97.57 ± 0.06</u>	<u>97.76 ± 0.05</u>
	Avg. Rank	6.08	6.00	6.33	4.42	8.42	6.92	6.58	4.92	<u>3.00</u>	<u>2.33</u>
ind	Wikipedia	75.65 ± 0.79	70.21 ± 1.58	87.00 ± 0.16	85.62 ± 0.44	74.06 ± 2.62	80.63 ± 0.00	86.76 ± 0.72	<u>88.59 ± 0.17</u>	78.29 ± 5.38	<u>87.06 ± 0.86</u>
	Reddit	86.98 ± 0.16	86.30 ± 0.26	89.59 ± 0.24	88.10 ± 0.24	<u>91.67 ± 0.24</u>	85.48 ± 0.00	87.45 ± 0.29	85.26 ± 0.11	91.11 ± 0.40	<u>91.77 ± 0.46</u>
	MOOC	65.23 ± 2.19	61.66 ± 0.95	75.95 ± 0.64	77.50 ± 2.91	73.51 ± 0.94	49.43 ± 0.00	74.65 ± 0.54	74.27 ± 0.92	<u>81.24 ± 0.69</u>	<u>81.19 ± 2.02</u>
	LastFM	62.67 ± 4.49	64.41 ± 2.70	71.13 ± 0.17	65.95 ± 5.98	67.48 ± 0.77	<u>75.49 ± 0.00</u>	58.21 ± 0.89	68.12 ± 0.33	73.97 ± 0.50	<u>75.05 ± 0.40</u>
	Enron	68.96 ± 0.98	67.79 ± 1.53	63.94 ± 1.36	70.89 ± 2.72	75.15 ± 0.58	73.89 ± 0.00	71.29 ± 0.32	75.01 ± 0.79	<u>77.41 ± 0.89</u>	<u>77.46 ± 0.90</u>
	Social Evo.	89.82 ± 4.11	93.28 ± 0.48	94.84 ± 0.44	95.13 ± 0.56	88.32 ± 0.27	83.69 ± 0.00	94.90 ± 0.36	94.72 ± 0.33	<u>97.68 ± 0.10</u>	<u>97.78 ± 0.15</u>
	UCI	65.99 ± 1.40	54.79 ± 1.76	68.67 ± 0.84	70.94 ± 0.71	64.61 ± 0.48	57.43 ± 0.00	76.01 ± 1.11	<u>80.10 ± 0.51</u>	72.25 ± 1.71	<u>77.75 ± 1.56</u>
	Can. Parl.	48.42 ± 0.66	58.61 ± 0.86	68.82 ± 1.21	65.34 ± 2.87	67.75 ± 1.00	62.16 ± 0.00	65.85 ± 1.75	69.48 ± 0.63	<u>95.44 ± 0.57</u>	<u>97.29 ± 0.96</u>
	US Legis.	50.27 ± 5.13	<u>83.44 ± 1.16</u>	61.91 ± 5.82	67.57 ± 6.47	65.81 ± 8.52	64.74 ± 0.00	78.15 ± 3.34	79.63 ± 0.84	81.25 ± 3.62	<u>85.61 ± 1.66</u>
	UN Trade	60.42 ± 1.48	60.19 ± 1.24	60.61 ± 1.24	61.04 ± 6.01	<u>62.54 ± 0.67</u>	<u>72.97 ± 0.00</u>	61.06 ± 1.74	60.15 ± 1.29	55.79 ± 1.02	60.43 ± 1.59
	UN Vote	<u>67.79 ± 1.46</u>	<u>67.53 ± 1.98</u>	52.89 ± 1.61	67.63 ± 2.67	52.19 ± 0.34	66.30 ± 0.00	50.62 ± 0.82	51.60 ± 0.73	51.91 ± 0.84	60.05 ± 2.41
	Contact	93.43 ± 1.78	94.18 ± 0.10	94.35 ± 0.48	90.18 ± 3.28	89.31 ± 0.27	85.20 ± 0.00	91.35 ± 0.21	90.87 ± 0.35	<u>94.75 ± 0.28</u>	<u>94.63 ± 0.06</u>
	Avg. Rank	7.33	7.25	5.25	5.17	6.17	6.75	5.67	5.42	<u>3.83</u>	<u>2.17</u>

**Figure 5: Ablation Studies for DyG-Mamba in both (A-B) transductive and (C-D) inductive settings.**

Ablation Study. To evaluate the effectiveness of irregular time-aware continuous SSMS, the selective mechanism, and the cross-attention layer, we conduct ablation studies with the following three variants: (i) w/o Time-span: we use the input data as control signals instead of time-spans, *i.e.*, $\Delta t = \text{SiLU}(\text{Linear}(\mathbf{u}(t)))$; (ii) w/o Selective: following the same parameter settings of S4 [13], *i.e.*, all parameters are irrelevant with input data or time-spans; and (iii) w/o Cross-attn: we remove the linear cross-attention layer. In Figure 5, we observe that the removal of either component of DyG-Mamba negatively impacts the ability of dynamic graph learning.

Specifically, compared to time-dependent DyG-Mamba, the performance of data-dependent w/o Time-span decreases significantly, especially in the inductive setting, showing the effectiveness of time-spans as control signals. Secondly, w/o Selective decreases the performance since the parameters are fixed and cannot fit to dynamic networks well. Finally, the cross-attention layer also brings a certain degree of performance gain.

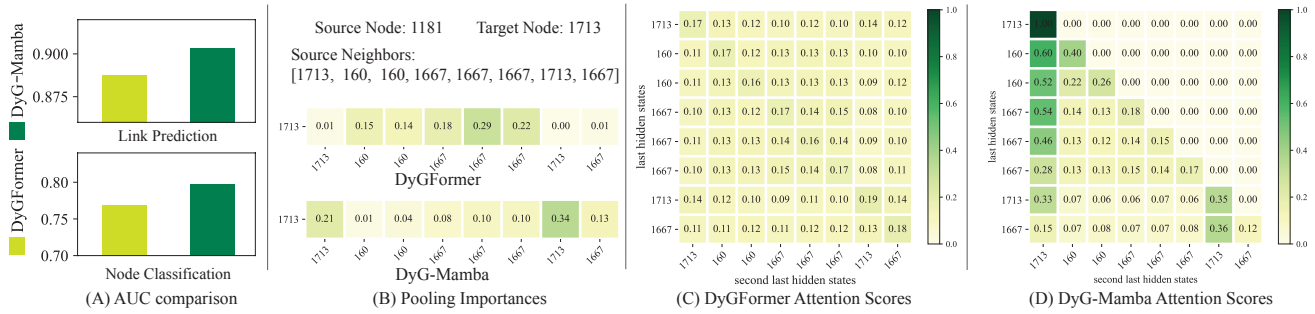


Figure 6: (A) Average AUC comparison. (B-D) An case study of historical attention mapping in DyG-Mamba and DyGFormer.

5.2 Qualitative Evaluation

Sensitivity to Sequence Length. To show the ability to capture long-term dependencies of DyG-Mamba, we select three best-performing baselines and depict their performance changing with varying sequence lengths in Figure 7. We observe that the performance of DyG-Mamba significantly improves with the increase of the sequence length, showing its ability for long sequence modeling. DyG-Mamba achieves better performance even with short sequence lengths, showing its ability on dynamic graph learning.

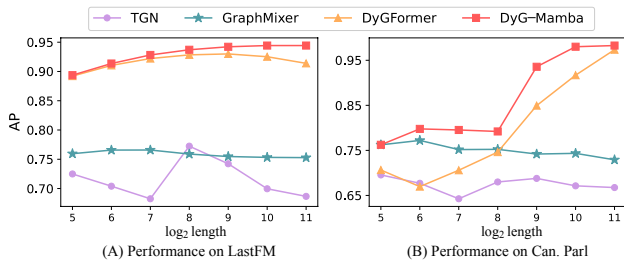


Figure 7: Performance with varying sequence lengths.

Robustness against Noise. We conduct robust tests by randomly inserting 10% to 60% noisy edges with chronological timestamps during the evaluation step. In Figure 8, as the noisy edges increase, DyG-Mamba performance decreases to a minimum extent, indicating that DyG-Mamba has stronger robustness than baselines. This is because DyG-Mamba adopts a selective mechanism that helps select the most relevant content and remove irrelevant information.

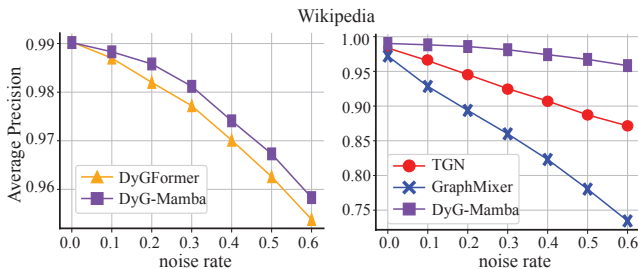


Figure 8: Robustness against noise, ranging from 0.1 to 0.6.

Time information Analysis. To evaluate the effectiveness of time information in DyG-Mamba, we conduct additional ablation studies, as shown in Table 5. There are four settings of DyG-Mamba:

(i) [w/o Time-Encoding] refers to removing time encoding $Z_{u,T}^T$; (ii) [w/o Time-Span] replaces time-span with data-dependent control signals; (iii) [w/o both Time] refers to removing both time-encoding and time-span; (iv) [all Time-dependent] set parameters B and C from data-dependent to time-span dependent. From the above Table 5, we observe that time information plays a crucial role in DyG-Mamba. Specifically, the Time-span is key to capturing irregular temporal patterns, which is essential for the overall performance. Additionally, the time-encoding, which captures the relative time to the current time, also contributes to performance improvement, although to a lesser extent. Finally, although the time-span is crucial for capturing temporal information, the model entirely time-dependent will significantly reduce performance.

Table 5: Results (AP score) of time information ablations.

Settings	Can. Parl.	Enron	UCI	USLegis.
w/o Time-encoding	97.80±0.43	92.83±0.06	95.92±0.11	73.33±1.15
w/o Time-span	96.90±0.18	92.14±0.12	95.62±0.05	72.26±0.76
w/o both Time	96.87±0.18	92.08±0.12	95.54±0.08	72.19±0.72
all Time-dependent	79.24±0.58	82.25±0.16	94.16±0.66	70.57±0.84
DyG-Mamba	98.20±0.52	93.14±0.08	96.14±0.14	73.66±1.13

Attention Investigation. We conduct a case study to reveal the attention mapping in DyG-Mamba. We aim to predict the link between nodes 1181 and 1713. Figure 6(B) show the normalized cosine similarity between the target node encoding and the last hidden state in each model with respect to source node’s neighbors. We observe that DyG-Mamba can better balance historical memory with current input, *i.e.*, it has higher similarity when input node 1713 is the source node’s neighbor. Figures 6(C)-(D) depict the normalized cosine similarity between the last hidden state and the second-to-last hidden state in each model. DyGFormer in Figures 6(C)-(D) exhibits the highest similarity along the diagonal and an almost uniform distributed similarity across all neighbors, indicating that it struggles to distinguish the correct node. In contrast, DyG-Mamba prioritizes important information and assigns higher scores to the target node, showing the effectiveness of its selective mechanism.

6 Conclusion

In this work, we proposed a new SSM-based framework, DyG-Mamba, designed to effectively and efficiently capture long-term temporal dependencies on dynamic graphs. To achieve this goal,

we directly used irregular time-spans as controllable signals to establish a strong correlation between dynamic evolution laws and time information, further improving the model's generalization and robustness. By evaluating on various downstream tasks, DyG-Mamba showed strong performance and applicability. We plan to apply DyG-Mamba to real-world applications in the future. In the future, we plan to design a more general framework based on DyG-Mamba to be applied to many real-world applications.

References

- [1] Unai Alvarez-Rodriguez, Federico Battiston, Guilherme Ferraz de Arruda, Yamir Moreno, Matjaž Perc, and Vito Latora. 2021. Evolutionary dynamics of higher-order interactions in social networks. *Nature Human Behaviour* 5, 5 (2021), 586–595.
- [2] Lei Bai, Lina Yao, Can Li, Xianzhi Wang, and Can Wang. 2020. Adaptive Graph Convolutional Recurrent Network for Traffic Forecasting. In *Advances in Neural Information Processing Systems* 33.
- [3] Djork-Arné Clevert, Thomas Unterthiner, and Sepp Hochreiter. 2016. Fast and Accurate Deep Network Learning by Exponential Linear Units (ELUs). In *4th International Conference on Learning Representations, ICLR 2016, San Juan, Puerto Rico, May 2–4, 2016, Conference Track Proceedings*, Yoshua Bengio and Yann LeCun (Eds.). <http://arxiv.org/abs/1511.07289>
- [4] Weilin Cong, Jian Kang, Hanghang Tong, and Mehrdad Mahdavi. 2024. On the Generalization Capability of Temporal Graph Learning Algorithms: Theoretical Insights and a Simpler Method. *CoRR* abs/2402.16387 (2024). <https://doi.org/10.48550/ARXIV.2402.16387> arXiv:2402.16387
- [5] Weilin Cong, Yanhong Wu, Yuandong Tian, Mengting Gu, Yinglong Xia, Mehrdad Mahdavi, and Chun-cheng Jason Chen. 2021. Dynamic Graph Representation Learning via Graph Transformer Networks. *CoRR* abs/2111.10447 (2021).
- [6] Weilin Cong, Si Zhang, Jian Kang, Baichuan Yuan, Hao Wu, Xin Zhou, Hanghang Tong, and Mehrdad Mahdavi. 2023. Do We Really Need Complicated Model Architectures For Temporal Networks?. In *International Conference on Learning Representations*.
- [7] Hermann Ebbinghaus. 1885. *Über das Gedächtnis: untersuchungen zur experimentellen psychologie*. Duncker & Humblot.
- [8] Yuan Feng, Yukun Cao, Wang Hairu, Xike Xie, and S Kevin Zhou. 2024. Mayfly: a Neural Data Structure for Graph Stream Summarization. In *The Twelfth International Conference on Learning Representations*. <https://openreview.net/forum?id=n7Sr8SW4bn>
- [9] Daniel Y Fu, Tri Dao, Khaled Kamal Saab, Armin W Thomas, Atri Rudra, and Christopher Re. 2022. Hungry Hungry Hippos: Towards Language Modeling with State Space Models. In *ICLR*.
- [10] Albert Gu and Tri Dao. 2023. Mamba: Linear-time sequence modeling with selective state spaces. *arXiv preprint arXiv:2312.00752* (2023).
- [11] Albert Gu, Tri Dao, Stefano Ermon, Atri Rudra, and Christopher Ré. 2020. HiPPO: Recurrent Memory with Optimal Polynomial Projections. In *Advances in Neural Information Processing Systems 33: Annual Conference on Neural Information Processing Systems 2020, NeurIPS 2020, December 6–12, 2020, virtual*, Hugo Larochelle, Marc'Aurelio Ranzato, Raia Hadsell, Maria-Florina Balcan, and Hsuan-Tien Lin (Eds.). <https://proceedings.neurips.cc/paper/2020/hash/102f0bb6efb3a6128a3c750dd16729be-Abstract.html>
- [12] Albert Gu, Tri Dao, Stefano Ermon, Atri Rudra, and Christopher Ré. 2020. Hippo: Recurrent memory with optimal polynomial projections. *NeurIPS* 33 (2020), 1474–1487.
- [13] Albert Gu, Karan Goel, and Christopher Ré. 2022. Efficiently Modeling Long Sequences with Structured State Spaces. In *The Tenth International Conference on Learning Representations*. OpenReview.net. <https://openreview.net/forum?id=uYLFoz1v1AC>
- [14] Albert Gu, Isys Johnson, Karan Goel, Khaled Saab, Tri Dao, Atri Rudra, and Christopher Ré. 2021. Combining Recurrent, Convolutional, and Continuous-time Models with Linear State Space Layers. In *Advances in Neural Information Processing Systems* 34. 572–585. <https://proceedings.neurips.cc/paper/2021/hash/05546b0e38ab9175cd905eebc6eb76-Abstract.html>
- [15] Shengnan Guo, Youfang Lin, Ning Feng, Chao Song, and Huaiyu Wan. 2019. Attention Based Spatial-Temporal Graph Convolutional Networks for Traffic Flow Forecasting. In *The Thirty-Third AAAI Conference on Artificial Intelligence*. AAAI Press, 922–929.
- [16] Ankit Gupta, Albert Gu, and Jonathan Berant. 2022. Diagonal State Spaces are as Effective as Structured State Spaces. In *Advances in Neural Information Processing Systems* 35. http://papers.nips.cc/paper_files/paper/2022/hash/9156b0f6dfa9bbd18c79cc459ef5d61c-Abstract-Conference.html
- [17] Ramin Hasani, Mathias Lechner, Tsun-Hsuan Wang, Makram Chahine, Alexander Amini, and Daniela Rus. 2022. Liquid Structural State-Space Models. In *ICLR*.
- [18] Sepp Hochreiter and Jürgen Schmidhuber. 1997. Long short-term memory. *Neural computation* 9, 8 (1997), 1735–1780.
- [19] Shenyang Huang, Samy Coulombe, Yasmeen Hitti, Reihaneh Rabbany, and Guillaume Rabusseau. 2024. Laplacian Change Point Detection for Single and Multi-view Dynamic Graphs. *ACM Trans. Knowl. Discov. Data* 18, 3 (2024), 63:1–63:32. <https://doi.org/10.1145/3631609>
- [20] Shenyang Huang, Farimah Poursafaei, Jacob Danovitch, Matthias Fey, Weihua Hu, Emanuele Rossi, Jure Leskovec, Michael M. Bronstein, Guillaume Rabusseau, and Reihaneh Rabbany. 2023. Temporal Graph Benchmark for Machine Learning on Temporal Graphs. In *Advances in Neural Information Processing Systems* 36. http://papers.nips.cc/paper_files/paper/2023/hash/066b98e633162f6562b35962671288-Abstract-Datasets_and_Benchmarks.html
- [21] Zijie Huang, Yizhou Sun, and Wei Wang. 2020. Learning Continuous System Dynamics from Irregularly-Sampled Partial Observations. In *Advances in Neural Information Processing Systems* 33.
- [22] Zihang Jiang, Weihao Yu, Daquan Zhou, Yunpeng Chen, Jiashi Feng, and Shuicheng Yan. 2020. ConvBERT: Improving BERT with Span-based Dynamic Convolution. In *Advances in Neural Information Processing Systems* 33. <https://proceedings.neurips.cc/paper/2020/hash/96da2f590cd7246bbde0051047b0d6f7-Abstract.html>
- [23] Ming Jin, Yuan-Fang Li, and Shirui Pan. 2022. Neural Temporal Walks: Motif-Aware Representation Learning on Continuous-Time Dynamic Graphs. In *Advances in Neural Information Processing Systems* 35. http://papers.nips.cc/paper_files/paper/2022/hash/7dad855cef7494d5d956a8d28add871-Abstract-Conference.html
- [24] Rudolph Emil Kalman. 1960. A new approach to linear filtering and prediction problems. (1960).
- [25] Angelos Katharopoulos, Apoorv Vyas, Nikolaos Pappas, and François Fleuret. 2020. Transformers are RNNs: Fast autoregressive transformers with linear attention. In *International Conference on Machine Learning*. PMLR, 5156–5165.
- [26] Diederik P. Kingma and Jimmy Ba. 2015. Adam: A Method for Stochastic Optimization. In *3rd International Conference on Learning Representations*.
- [27] Srijan Kumar, Xikun Zhang, and Jure Leskovec. 2019. Predicting dynamic embedding trajectory in temporal interaction networks. In *Proceedings of the 25th ACM SIGKDD International Conference on Knowledge Discovery & Data Mining*.
- [28] Jay H Lee, Manfred Morari, and Carlos E Garcia. 1994. State-space interpretation of model predictive control. *Automatica* 30, 4 (1994), 707–717.
- [29] Lincan Li, Hanchen Wang, Wenjie Zhang, and Adelle Coster. 2024. STG-Mamba: Spatial-Temporal Graph Learning via Selective State Space Model. arXiv:2403.12418 [cs.LG]
- [30] Meng Liu, Yue Liu, KE LIANG, Wenxuan Tu, Siwei Wang, Sihang Zhou, and Xinwang Liu. 2024. Deep Temporal Graph Clustering. In *The Twelfth International Conference on Learning Representations*. <https://openreview.net/forum?id=ViNe1fjGME>
- [31] Antonio Longa, Veronica Lachi, Gabriele Santin, Monica Bianchini, Bruno Lepri, Pietro Lio, franco scarselli, and Andrea Passerini. 2023. Graph Neural Networks for Temporal Graphs: State of the Art, Open Challenges, and Opportunities. *Transactions on Machine Learning Research* (2023). <https://openreview.net/forum?id=pHCdMat0GI>
- [32] Linhao Luo, Gholamreza Haffari, and Shirui Pan. 2023. Graph Sequential Neural ODE Process for Link Prediction on Dynamic and Sparse Graphs. In *Proceedings of the Sixteenth ACM International Conference on Web Search and Data Mining*, Tat-Seng Chua, Hady W. Lauw, Luo Si, Evimaria Terzi, and Panayiotis Tsaparas (Eds.). ACM, 778–786. <https://doi.org/10.1145/3539597.3570465>
- [33] Xiao Luo, Haixin Wang, Zijie Huang, Huiyu Jiang, Abhijeet Sadashiv Gangan, Song Jiang, and Yizhou Sun. 2023. CARE: Modeling Interacting Dynamics Under Temporal Environmental Variation. In *Thirty-seventh Conference on Neural Information Processing Systems*. <https://openreview.net/forum?id=lgw3ohkFRv>
- [34] Chen Ma, Liheng Ma, Yingxue Zhang, Jianing Sun, Xue Liu, and Mark Coates. 2020. Memory Augmented Graph Neural Networks for Sequential Recommendation. In *The Thirty-Fourth AAAI Conference on Artificial Intelligence*. AAAI Press, 5045–5052. <https://doi.org/10.1609/AAAI.V34I04.5945>
- [35] Yao Ma, Ziyi Guo, Zhaochun Ren, Eric Zhao, Jiliang Tang, and Dawei Yin. 2018. Streaming graph neural networks. *arXiv:1810.10627* (2018).
- [36] Anmol Madan, Manuel Cebrian, Sai Moturu, Katayoun Farrahi, et al. 2011. Sensing the "health state" of a community. *IEEE Pervasive Computing* 11, 4 (2011).
- [37] Prabhaker Mishra, Uttam Singh, Chandra M Pandey, Priyadarshni Mishra, and Gaurav Pandey. 2019. Application of student's t-test, analysis of variance, and covariance. *Annals of cardiac anaesthesia* 22, 4 (2019), 407–411.
- [38] Vinod Nair and Geoffrey E. Hinton. 2010. Rectified Linear Units Improve Restricted Boltzmann Machines. In *Proceedings of the 27th International Conference on Machine Learning*. Omnipress, 807–814.
- [39] Pietro Panzarasa, Tore Opsahl, and Kathleen M Carley. 2009. Patterns and dynamics of users' behavior and interaction: Network analysis of an online community. *Journal of the American Society for Information Science and Technology* 60, 5 (2009), 911–932.
- [40] Aldo Pareja, Giacomo Domeniconi, Jie Chen, Tengfei Ma, Toyotaro Suzumura, Hiroki Kanezashi, Tim Kaler, Tao B. Schardl, and Charles E. Leiserson. 2020.

- EvolveGCN: Evolving Graph Convolutional Networks for Dynamic Graphs. In *The Thirty-Fourth AAAI Conference on Artificial Intelligence*. AAAI Press, 5363–5370.
- [41] Jong Ho Park, Jaden Park, Zheyang Xiong, Nayoung Lee, Jaewoong Cho, Samet Oymak, Kangwook Lee, and Dimitris Papailiopoulos. 2024. Can Mamba Learn How To Learn? A Comparative Study on In-Context Learning Tasks. In *International Conference on Machine Learning, ICML (Proceedings of Machine Learning Research)*.
- [42] James W Pennebaker, Martha E Francis, and Roger J Booth. 2001. Linguistic inquiry and word count: LIWC 2001. *Mahway: Lawrence Erlbaum Associates* 71, 2001 (2001), 2001.
- [43] Farimah Poursafaei, Andy Huang, Kellin Pelrine, and Reihaneh Rabbany. 2022. Towards Better Evaluation for Dynamic Link Prediction. In *Thirty-sixth Conference on Neural Information Processing Systems Datasets and Benchmarks Track*.
- [44] Emanuele Rossi, Ben Chamberlain, Fabrizio Frasca, Davide Eynard, Federico Monti, and Michael Bronstein. 2020. Temporal Graph Networks for Deep Learning on Dynamic Graphs. In *ICML 2020 Workshop on Graph Representation Learning*.
- [45] Aravind Sankar, Yanhong Wu, Liang Gou, Wei Zhang, and Hao Yang. 2020. DySAT: Deep Neural Representation Learning on Dynamic Graphs via Self-Attention Networks. In *The Thirteenth ACM International Conference on Web Search and Data Mining*. ACM, 519–527.
- [46] Youngjoon Seo, Michaël Defferrard, Pierre Vandergheynst, and Xavier Bresson. 2018. Structured Sequence Modeling with Graph Convolutional Recurrent Networks. In *Neural Information Processing - 25th International Conference (Lecture Notes in Computer Science, Vol. 11301)*. Springer, 362–373. https://doi.org/10.1007/978-3-030-04167-0_33
- [47] Jitesh Shetty and Jafar Adibi. 2004. The Enron email dataset database schema and brief statistical report. *Information sciences institute technical report, University of Southern California* 4, 1 (2004), 120–128.
- [48] Jimmy TH Smith, Andrew Warrington, and Scott Linderman. 2022. Simplified State Space Layers for Sequence Modeling. In *ICLR*.
- [49] Weiping Song, Zhiping Xiao, Yifan Wang, Laurent Charlin, Ming Zhang, and Jian Tang. 2019. Session-Based Social Recommendation via Dynamic Graph Attention Networks. In *Proceedings of the Twelfth ACM International Conference on Web Search and Data Mining*. ACM, 555–563.
- [50] Yujin Tang, Peijie Dong, Zhenheng Tang, Xiaowen Chu, and Junwei Liang. 2024. VMRNN: Integrating Vision Mamba and LSTM for Efficient and Accurate Spatiotemporal Forecasting. *arXiv preprint arXiv:2403.16536* (2024).
- [51] Yuxing Tian, Yiyang Qi, and Fan Guo. 2024. FreeDyG: Frequency Enhanced Continuous-Time Dynamic Graph Model for Link Prediction. In *The Twelfth International Conference on Learning Representations*. <https://openreview.net/forum?id=82Mc5illnM>
- [52] Ilya O. Tolstikhin, Neil Houlsby, Alexander Kolesnikov, Lucas Beyer, Xiaohua Zhai, Thomas Unterthiner, Jessica Yung, Andreas Steiner, Daniel Keysers, Jakob Uszkoreit, Mario Lucic, and Alexey Dosovitskiy. 2021. MLP-Mixer: An all-MLP Architecture for Vision. In *Advances in Neural Information Processing Systems* 34, 24261–24272.
- [53] Rakshit Trivedi, Mehrdad Farajtabar, Prasenjeet Biswal, and Hongyuan Zha. 2019. DyRep: Learning Representations over Dynamic Graphs. In *7th International Conference on Learning Representations*. OpenReview.net.
- [54] Ashish Vaswani, Noam Shazeer, Niki Parmar, Jakob Uszkoreit, Llion Jones, Aidan N. Gomez, Lukasz Kaiser, and Illia Polosukhin. 2017. Attention is All you Need. In *Advances in Neural Information Processing Systems*. 5998–6008.
- [55] Chloe Wang, Oleksii Tsepa, Jun Ma, and Bo Wang. 2024. Graph-Mamba: Towards Long-Range Graph Sequence Modeling with Selective State Spaces. *CoRR* abs/2402.00789 (2024). <https://doi.org/10.48550/ARXIV.2402.00789> arXiv:2402.00789
- [56] Lu Wang, Xiaofu Chang, Shuang Li, Yunfei Chu, Hui Li, Wei Zhang, Xiaofeng He, Le Song, Jingren Zhou, and Hongxia Yang. 2021. TCL: Transformer-based Dynamic Graph Modelling via Contrastive Learning. *CoRR* abs/2105.07944 (2021).
- [57] Sinong Wang, Belinda Z. Li, Madian Khabsa, Han Fang, and Hao Ma. 2020. Linformer: Self-Attention with Linear Complexity. *CoRR* abs/2006.04768 (2020). arXiv:2006.04768
- [58] Yanbang Wang, Yen-Yu Chang, Yunyu Liu, Jure Leskovec, and Pan Li. 2021. Inductive Representation Learning in Temporal Networks via Causal Anonymous Walks. In *9th International Conference on Learning Representations*. OpenReview.net.
- [59] Yuxia Wu, Yuan Fang, and Lizi Liao. 2024. On the Feasibility of Simple Transformer for Dynamic Graph Modeling. In *Proceedings of the ACM on Web Conference 2024* (<conf-loc>, <city>Singapore</city>, <country>Singapore</country>, </conf-loc>) (WWW '24). Association for Computing Machinery, New York, NY, USA, 870–880. <https://doi.org/10.1145/3589334.3645622>
- [60] Da Xu, Chuanwei Ruan, Evren Körpeoglu, Sushant Kumar, and Kannan Achan. 2020. Inductive representation learning on temporal graphs. In *8th International Conference on Learning Representations*. OpenReview.net. <https://openreview.net/forum?id=rjEw1yHYwH>
- [61] Jiaxuan You, Tianyu Du, and Jure Leskovec. 2022. ROLAND: Graph Learning Framework for Dynamic Graphs. In *The 28th ACM SIGKDD Conference on Knowledge Discovery and Data Mining*. ACM, 2358–2366.
- [62] Le Yu, Zihang Liu, Leilei Sun, Bowen Du, Chuanren Liu, and Weifeng Lv. 2023. Continuous-Time User Preference Modelling for Temporal Sets Prediction. *IEEE Transactions on Knowledge and Data Engineering* (2023).
- [63] Le Yu, Leilei Sun, Bowen Du, and Weifeng Lv. 2023. Towards Better Dynamic Graph Learning: New Architecture and Unified Library. In *Advances in Neural Information Processing Systems* 36.
- [64] Weihao Yu and Xinchao Wang. 2024. MambaOut: Do We Really Need Mamba for Vision? arXiv:2405.07992 [cs.CV]
- [65] Mengqi Zhang, Shu Wu, Xueli Yu, Qiang Liu, and Liang Wang. 2022. Dynamic graph neural networks for sequential recommendation. *IEEE Transactions on Knowledge and Data Engineering* (2022).
- [66] Lianghui Zhu, Bencheng Liao, Qian Zhang, Xinlong Wang, Wenyu Liu, and Xingang Wang. 2024. Vision mamba: Efficient visual representation learning with bidirectional state space model. *arXiv preprint arXiv:2401.09417* (2024).

A More Details about Related Works

A.1 Similarities and Differences Discussion

We are the first to apply SSMs (Mamba) to the dynamic graph domain and identify the reasons behind its poor performance. Here, we will discuss the differences between our approach and those of Mamba, DyGFormer, and TCL. We also provide both theoretical and experimental evidence demonstrating why it is efficient.

Compared to Vanilla Mamba [10]. Vanilla Mamba can provide high efficiency but shows limited effectiveness for dynamic graph modeling. We carefully analyze three core shortcomings of Mamba in dynamic graph modeling.

- A significant challenge to model continuous-time dynamic graphs is that interactions occur irregularly. Mamba lacks the ability to explore temporal information with irregular time intervals. Because Mamba simply concatenates node attributes with extra time encoding when aggregating the neighborhood information, which models temporal dependencies implicitly [23].
- Mamba has poor generalization in inductive scenarios with unseen nodes. The main contribution of Mamba, compared to previous Hippo and S4, is setting parameters as input data-dependent variables. However, real-world dynamic systems always have incoming unseen nodes, input data-dependent Mamba shows low generalization on them. While the DyG-Mamba designs irregular time-span control signals, which can extract more temporal information for selectively copy previous hidden states.
- Mambaout [64] argued that Mamba is suitable for auto-regressive tasks instead of classification tasks, and applying it to dynamic graphs is difficult. We also observe poor performance when directly applying vanilla Mamba for dynamic graph link prediction. Because it ignores the co-historical information between the pair of nodes for dynamic link prediction. The DyG-Mamba uses a shared encoder to generate two encodings separately and introduces a general linear cross-attention framework, which captures the co-historical information between two sequences.

Compared to DyGFormer [63] We use a unified continuous-time dynamic graph learning library (DyGLib) for a fair comparison. Consequently, we have the same input sequences, standard training pipelines, and evaluation strategies.

- DyG-Mamba adopts SSM-based causal attention to learn temporal node embedding, while DyGFormer adopts traditional Transformer encoder layers with a bi-directional self-attention mechanism.
- DyGFormer uses relative time encoding, which captures the time information from the current time and cannot capture irregular time-spans information. DyG-Mamba keeps the relative time encoding and treats the time intervals as the control signal to help the selection between historical and current sequence input.
- DyGFormer directly aggregates historical node embedding to obtain current node embedding. DyG-Mamba uses a shared encoder to generate two encodings separately and adds an additional linear cross-attention layer before aggregating for final node embeddings, which further improves the performance

by capturing the co-historical information between two target nodes.

- DyGFormer uses a patching technique for long sequences, which divides the encoding sequence into multiple non-overlapping patches. This will cause the loss of information as each patch shares one patch encoding. DyG-Mamba does not need a patching technique, since it can deal with long sequences in linear time and space complexity.

Compared our Cross-attention layer to TCL [56] We use a more efficient cross-attention layer to TCL. We all based on the idea that "the co-information of historical interaction between nodes" is important for the dynamic link prediction task.

- Considering the efficiency of the overall framework, we adopt a linear cross-attention layer. However, TCL directly uses the traditional cross-attention layer with quadratic time complexity.
- TCL uses additional FNN+ADD+LN layers in the middle of cross-attention, while DyG-Mamba only adopts one LN layer, which makes DyG-Mamba simple yet efficient.
- The linear cross-attention layer in DyG-Mamba plays the role of readout function for the final sequence embedding, while TCL stacks the standard attention and the cross-attention to attend nodes within and between sequences. This is a complex design, but similar to directly concatenating two sequences into one and encoding it by standard attention.

A.2 More Related Works

Dynamic Graph Learning. Representation learning on dynamic graphs has recently attracted great attention [8, 20, 30, 31]. *Discrete-time methods* manually divide the dynamic graph into a sequence of snapshots with different resolutions (one day/an hour) and then combine GNN (snapshot encoder) with recurrent models (dynamic tracker) to learn the representation of nodes [5, 40, 45, 46, 56, 61]. The main drawback of them is the necessity to predetermine the time granularity to create snapshots, ignoring the fine-grained temporal order of nodes/edges within each snapshot [58, 63]. In contrast, *continuous-time methods* directly use timestamps for representation learning. Based on neural architectures, we classify them into four main classes. Specifically, *RNN-based methods*, e.g., JODIE [27] and TGN [44], first aggregate node's neighbors as current node representation and then update them using recurrent units [35, 53]. *GNN-based methods*, e.g., TGAT [58] and DySAT [45], obtain node representation using the graph attention mechanism for weighted aggregation of its short-term (always 20) temporal neighbors. *MLP-based methods*, e.g., GraphMixer [6] and FreeDyG [51], learn node representation by directly aggregating its temporal neighbors with MLP-Mixer [52], where short-term neighbor lengths (10~30) yield better performance. *Transformer-based methods*, e.g., SimpleDyG [59] and DyGFormer [63], adopt self-attention for node's neighbor sequence and aggregates neighbors' hidden vectors as node's representation. Building upon these architectures, other methods incorporate additional techniques, such as ordinary differential equations [32, 33], random walks [23, 58] and temporal point process [19, 21], to effectively learn the continuous temporal information for some specific tasks. The differences between our work and the previous dynamic graph learning methods lie in two points.

First, while Transformers and RNNs face unaffordable computational costs or optimization issues (e.g., vanishing/exploding gradients), our method effectively captures the long-term dependency by leveraging the inherent advantages of the Mamba architecture. Second, our method utilizes the irregular timestamps to enhance the model’s ability to control the balance between historical state and current input.

State Space Models (SSMs), Originating from control systems [24, 28], SSMs inspire great attention for long-sequence modeling with HiPPO initialization [12, 14]. To enhance computational efficiency, Structured state space models (S4) normalizes the parameters into diagonal structure [13]. Since then, many flavors of structured state space models sprang up, e.g., parallel scan (S5) [48], shift SSM for linear attention (H3) [9] and diagonal structure design for parameters [17]. To remove linear time invariance constraint for better generalization, Mamba introduces a data-dependent selection mechanism to S4 to capture long-range context with increasing sequence length and a hardware-aware algorithm for efficient implementation [10]. Benefiting from its linear-time efficiency in long-sequence modeling, emerging works are proposed and outperforms Transformers on various benchmarks [41, 50, 66], while few work focuses on graph domain. Graph-Mamba [55] selectively samples node neighbors on large-scale graphs using graph-centric node prioritization and permutation strategies to enhance context-aware reasoning, and then aggregates selected neighbors’ information for node representation learning. STG-Mamba [29] proposes Kalman Filtering GNNs for adaptive graph structure upgrading of snapshots and adopts Mamba layers to capture the dynamic evolution of spatial-temporal graphs. Different from Graph-Mamba and STG-Mamba, we consider continuous-time dynamic graph modeling while they focus on static graph or snapshots. Furthermore, STG-Mamba only focus on graph generation task with MES loss while we aims to build a general continuous SSM backbone, which can be adopted on any dynamic graph tasks.

A.3 Descriptions of Baselines

JODIE [27]: focuses on bipartite networks of instantaneous user-item interactions. JODIE has an update operation and a projection operation. The former utilizes two coupled RNNs to recursively update the representation of the users and items. The latter predicts the future representation of a node, while considering the elapsed time since its last interaction.

DyRep [53]: has a custom RNN that updates node representations upon observation of a new edge. For obtaining the neighbor weights at each time, DyRep uses a temporal attention mechanism which is parameterized by the recurrent architecture.

TGAT [60]: aggregates features of temporal-topological neighborhood and temporal interactions of dynamic network. The proposes TGAT layer employs a modified self-attention mechanism as its building block where the positional encoding module is replaced by a functional time encoding.

TGN [44]: consists of five main modules: (1) *memory*: containing each node’s history and is used to store long-term dependencies, (2) *message function*: for updating the memory of each node based on the messages that are generated upon observation of an event, (3)

message aggregator: aggregating several message involving a single node, (4) *memory updater*: responsible for updating the memory of a node according to the aggregated messages, and (5) *embedding*: generating the representations of the nodes using the node’s memory as well as the node and edge features. Similar to TGAT, TGN also utilizes time encoding for effectively capturing the inter-event temporal information.

CAWN [58]: generates several Causal Anonymous Walks (CAWs) for each node, and uses these CAWs to generate relative node identities. The identities together with the encoded elapsed time are used for encoding the CAWs by an RNN. Finally, the encodings of several CAWs are aggregated and fed to a MLP for predicting the probability of a link between two nodes.

EdgeBank [43]: is a simple memory-based heuristic approach without any learning component for dynamic link prediction. EdgeBank simply stores observed edges in a memory, and then predicts True if the queried node pair is in the memory, otherwise predicts False. The strategy for storing observed edges has four variants including EdgeBank_∞ stores all the observed edges; EdgeBank_{tw-ts} and EdgeBank_{tw-te} remember edges within a fixed-size time window from the immediate past; EdgeBank_{th} retains edges with appearing counts higher than a threshold. We experiment with all four variants and report the best performance among them. Since EdgeBank is a heuristic approach, it costs no GPU memory.

TCL [56]: employs Transformer module to generate temporal neighborhood representations for nodes involved in nodes. And then use a co-attentional transformer to capture the inter-dependencies between neighborhoods of node pairs at a semantic level. Specifically, TCL generates each node’s interaction sequence by performing a breadth-first search algorithm on the temporal dependency interaction sub-graph.

GraphMixer [6]: shows that a fixed time encoding function performs better than the trainable version. It is a simple model for dynamic link prediction consisting of three main modules: a node-encoder to summarize the node information, a link-encoder to summarize the temporal link information, and a link predictor module. These modules that only employ based on MLP-Mixer [52] to learn from temporal links.

DyGFormer [63]: is a new Transformer-based architecture, which proposes a neighbor co-occurrence encoding scheme to exploit the correlations of nodes in each interaction. DyGFormer concatenates the source sequence and target sequence into a longer sequence, then utilizes transformer encoders to capture the inter-dependencies between two sequences. Even DyGFormer achieves a great performance, the $O(L^2)$ time/space complexity makes it hard to scale up the sequence length. Therefore, DyGFormer applies a patching technique to shorten the sequence length.

B Proofs for Theorems

B.1 Proofs of Theorem 1

Starting with the linear time-invariant ODE function of the following form:

$$\frac{d}{dt}\mathbf{h}(t) = \mathbf{A}\mathbf{h}(t) + \mathbf{B}\mathbf{u}(t) \quad (15)$$

where $\mathbf{u}(t)$ is the input function and $\mathbf{h}(t)$ represents hidden state.

We prove $\mathbf{h}(t + \Delta t) = \bar{\mathbf{A}}\mathbf{h}(t) + \bar{\mathbf{B}}\mathbf{u}(t)$, if $\bar{\mathbf{A}} = e^{A\Delta t}$ and $\bar{\mathbf{B}} = (\Delta t \mathbf{A})^{-1} (e^{A\Delta t} - \mathbf{I}) (\Delta t \mathbf{B})$ under the assumption of zero-order hold (ZOH). The ZOH method assumes that $\mathbf{u}(t)$ is constant during each time interval Δt , which means $\mathbf{u}(t + \gamma) = \mathbf{u}(t)$ if $\gamma < \Delta t$. This is used to the derivation of Eq.(22). By multiplying both sides of the ODE equation by e^{-At} , we have:

$$e^{-At} \frac{d}{dt}\mathbf{h}(t) = e^{-At} \mathbf{A}\mathbf{h}(t) + e^{-At} \mathbf{B}\mathbf{u}(t) \quad (16)$$

$$\iff \frac{d}{dt}(e^{-At}\mathbf{h}(t)) = e^{-At} \mathbf{B}\mathbf{u}(t), \quad (17)$$

by integrating, we could prove

$$e^{-At}\mathbf{h}(t) - e^0\mathbf{h}(0) = \int_0^t e^{-A\tau} \mathbf{B}\mathbf{u}(\tau) d\tau, \quad (18)$$

From Eq. 18, we could prove $\mathbf{h}(t) = e^{At}\mathbf{h}(0) + \int_0^t e^{A(t-\tau)} \mathbf{B}\mathbf{u}(\tau) d\tau$. Following we will prove $\mathbf{h}(t + \Delta t)$.

$$\mathbf{h}(t + \Delta t) = e^{A(t+\Delta t)}\mathbf{h}(0) + \int_0^{t+\Delta t} e^{A(t+\Delta t-\tau)} \mathbf{B}\mathbf{u}(\tau) d\tau \quad (19)$$

$$= e^{At} e^{A(\Delta t)}\mathbf{h}(0) + e^{A(\Delta t)} \left(\int_0^t e^{A(t-\tau)} \mathbf{B}\mathbf{u}(\tau) d\tau + \int_0^{\Delta t} e^{A(t-\tau)} \mathbf{B}\mathbf{u}(\tau) d\tau \right) \quad (20)$$

$$= e^{A\Delta t} \left(e^{At}\mathbf{h}(0) + \int_0^t e^{A(t-\tau)} \mathbf{B}\mathbf{u}(\tau) d\tau \right) + \int_0^{\Delta t} e^{A(t+\Delta t-\tau)} \mathbf{B}\mathbf{u}(\tau) d\tau \quad (21)$$

$$\frac{v(\tau)=t+\Delta t-\tau}{u(t+\tau)=u(t)} e^{A\Delta t}\mathbf{h}(t) - \left(\int_{v(t)}^{v(t+\Delta t)} e^{Av} dv \right) \mathbf{B}\mathbf{u}(t) \quad (22)$$

$$= e^{A\Delta t}\mathbf{h}(t) + \left(\int_0^{\Delta t} e^{Av} dv \right) \mathbf{B}\mathbf{u}(t) \quad (23)$$

$$= e^{A\Delta t}\mathbf{h}(t) + \mathbf{A}^{-1} (e^{A\Delta t} - \mathbf{I}) \mathbf{B}\mathbf{u}(t) \quad (24)$$

$$= e^{A\Delta t}\mathbf{h}(t) + (\Delta t \mathbf{A})^{-1} (e^{A\Delta t} - \mathbf{I}) (\Delta t \mathbf{B})\mathbf{u}(t) \quad (25)$$

$$= \bar{\mathbf{A}}\mathbf{h}(t) + \bar{\mathbf{B}}\mathbf{u}(t) \quad (26)$$

□

B.2 Proofs of Theorem 2

Let A be diagonalizable over \mathbb{C} as $A = V\Lambda V^{-1}$ with eigenvalues $\lambda_1, \dots, \lambda_N \in \mathbb{C}$. Given Δt_k , we first prove $\bar{\mathbf{A}}_k = \text{diag}(e^{\lambda_1 \Delta t_k}, \dots, e^{\lambda_N \Delta t_k})$ and $\bar{\mathbf{B}}_k = \left(\lambda_i^{-1} (e^{\lambda_i \Delta t_k} - 1) \right)_{1 \leq i \leq N}$. And, to make the proof clearer and easier to understand, we restate the definition of SSM.

SSM [10, 34, 41] defines a linear mapping from input $\mathbf{u}(t) \in \mathbb{R}^d$ to output $\mathbf{y}(t) \in \mathbb{R}^d$ through a state-variable $\mathbf{h}(t) \in \mathbb{R}^{m \times d}$, formulated by:

$$\mathbf{h}'(t) = \mathbf{A}\mathbf{h}(t) + \mathbf{B}\mathbf{u}(t), \quad \mathbf{y}(t) = \mathbf{C}\mathbf{h}(t) + \mathbf{D}\mathbf{u}(t), \quad (27)$$

where $\mathbf{A} \in \mathbb{R}^{m \times m}$, $\mathbf{B}, \mathbf{C} \in \mathbb{R}^m$ are the weighting trainable parameters, and \mathbf{D} always equals to 0. For application to a discrete input sequence $(\mathbf{u}_1, \mathbf{u}_2, \dots, \mathbf{u}_\tau)$ instead of a continuous function, Eq.(1) can be discredited with a step size Δ , indicating the input's resolution. Followed [10], we consider to discretize SSM using the zero-order hold (ZOH) discretization rule, which can be formulated by:

$$\mathbf{h}_t = \bar{\mathbf{A}}\mathbf{h}_{t-1} + \bar{\mathbf{B}}\mathbf{u}_t, \quad \mathbf{y}_t = \mathbf{C}\mathbf{h}_t, \quad (28)$$

$$\text{where } \bar{\mathbf{A}} = \exp(\Delta \mathbf{A}), \quad \bar{\mathbf{B}} = (\Delta \mathbf{A})^{-1} (\exp(\Delta \mathbf{A}) - \mathbf{I}) (\Delta \mathbf{B}).$$

By transforming the parameters from $(\Delta, \mathbf{A}, \mathbf{B})$ to $(\bar{\mathbf{A}}, \bar{\mathbf{B}})$, the SSM model becomes a sequence-to-sequence mapping framework from discrete input $\{\mathbf{u}_1, \mathbf{u}_2, \dots, \mathbf{u}_\tau\}$ to output $\{\mathbf{y}_1, \mathbf{y}_2, \dots, \mathbf{y}_\tau\}$. Then, the recurrence of Eq.(28) can be explicitly unrolled as

$$\mathbf{y}_k = \sum_{j=0}^k \overline{\mathbf{C}\mathbf{A}^k\mathbf{B}} \cdot \mathbf{u}_{k-j}. \quad (29)$$

For convenience, the scalars $\overline{\mathbf{C}\mathbf{A}^k\mathbf{B}}$ are gathered to define the SSM kernel $\bar{\mathbf{K}} \in \mathbb{R}^\tau$ as

$$\bar{\mathbf{K}} = (\overline{\mathbf{C}\mathbf{B}}, \overline{\mathbf{C}\mathbf{A}\mathbf{B}}, \dots, \overline{\mathbf{C}\mathbf{A}^{\tau-1}\mathbf{B}}) = (\mathbf{C}e^{\mathbf{A} \cdot k\Delta}(e^{\mathbf{A}\Delta} - \mathbf{I})\mathbf{A}^{-1}\mathbf{B})_{0 \leq k < \tau}, \quad (30)$$

where the last equality follows by substituting the values of $\bar{\mathbf{A}}, \bar{\mathbf{B}}, \bar{\mathbf{C}}$ from Equation (28). Hence,

$$\mathbf{y}_k = \sum_{j=0}^k \bar{\mathbf{K}}_j \cdot \mathbf{u}_{k-j}. \quad (31)$$

According to *Ankit Gupta et al.* [16], we have the following Proposition 1.

PROPOSITION 1. *Let $\mathbf{K} \in \mathbb{R}^{1 \times L}$ be the kernel of length L of a given state space $(\mathbf{A}, \mathbf{B}, \mathbf{C})$ and sample time $\Delta > 0$, where $\mathbf{A} \in \mathbb{C}^{N \times N}$ is diagonalizable over \mathbb{C} with eigenvalues $\lambda_1, \dots, \lambda_N$ and $\forall i, \lambda_i \neq 0$ and $e^{L\lambda_i\Delta} \neq 1$. Let $\mathbf{P} \in \mathbb{C}^{N \times L}$ be $\mathbf{P}_{i,k} = \lambda_i k\Delta$ and Λ be the diagonal matrix with $\lambda_1, \dots, \lambda_N$. Then there exist $\tilde{\mathbf{w}}, \mathbf{w} \in \mathbb{C}^{1 \times N}$ such that*

$$\mathbf{K} = \bar{\mathbf{K}}_{\Delta,L}(\Lambda, (1)_{1 \leq i \leq N}, \tilde{\mathbf{w}}) = \tilde{\mathbf{w}} \cdot \Lambda^{-1}(e^{\Lambda\Delta} - \mathbf{I}) \cdot \text{elementwise-exp}(\mathbf{P}), \quad (32)$$

As stated in Proposition 1, for this state space, *i.e.*, $\bar{\mathbf{K}}_{\Delta,L}(\Lambda, (1)_{1 \leq i \leq N}, \tilde{\mathbf{w}})$, and sample time Δ , we use Equation (28) to obtain its discretization

$$\bar{\mathbf{A}} = \text{diag}(e^{\lambda_1\Delta}, \dots, e^{\lambda_N\Delta}), \quad \bar{\mathbf{B}} = \left(\lambda_i^{-1}(e^{\lambda_i\Delta} - 1) \right)_{1 \leq i \leq N}$$

where diag creates a diagonal matrix of the scalars. We can now compute the states using the SSM recurrence $\mathbf{h}_k = \bar{\mathbf{A}}\mathbf{h}_{k-1} + \bar{\mathbf{B}}\mathbf{u}_k$ (Equation (28)). As $\bar{\mathbf{A}}$ is diagonal, the N coordinates do not interact and hence can be computed independently. Let us assume $\mathbf{h}_{-1} = 0$ and say we have already computed \mathbf{h}_{k-1} . Then, for the i 'th coordinate independently compute

$$\mathbf{h}_{i,k} = e^{\lambda_i\Delta}\mathbf{h}_{i,k-1} + \lambda_i^{-1}(e^{\lambda_i\Delta} - 1)\mathbf{u}_k.$$

B.3 Proofs of Theorem 3

Since DyG-Mamba has three core parameters, *i.e.*, Δ, \mathbf{B} and \mathbf{C} that control its effectiveness. We define Theorem 3 to explain the main effects of the parameters \mathbf{B} and \mathbf{C} .

We first copy Eq.(8) from the paper, SSM-based node representation learning process, as follows

$$\mathbf{h}_k = \bar{\mathbf{A}}_k\mathbf{h}_{k-1} + \bar{\mathbf{B}}_k\mathbf{u}_k, \quad \hat{\mathbf{z}}_k^\tau = \bar{\mathbf{C}}_k\mathbf{h}_k, \quad (33)$$

\mathbf{h}_k in Eq.(33) can be further decomposed as follows:

$$\mathbf{h}_k = \prod_{i=0}^{k-2} \bar{\mathbf{A}}_{k-i} \bar{\mathbf{B}}_1 \mathbf{u}_1 + \dots + \prod_{i=0}^{k-j} \bar{\mathbf{A}}_{k-i} \bar{\mathbf{B}}_{j-1} \mathbf{u}_{j-1} + \dots + \bar{\mathbf{B}}_k \mathbf{u}_k, \quad (34)$$

Then, considering \mathbf{A} is one fixed parameter and $\bar{\mathbf{A}}_k = \exp(\Delta t_k \mathbf{A})$, $\hat{\mathbf{z}}_k^\tau$ in Eq.(8) can be formulated as:

$$\begin{aligned} \hat{\mathbf{z}}_k^\tau &= \bar{\mathbf{C}}_k \prod_{i=0}^{k-2} \bar{\mathbf{A}}_{k-i} \bar{\mathbf{B}}_1 \mathbf{u}_1 + \dots + \bar{\mathbf{C}}_k \prod_{i=0}^{k-j} \bar{\mathbf{A}}_{k-i} \bar{\mathbf{B}}_{j-1} \mathbf{u}_{j-1} + \dots + \bar{\mathbf{C}}_k \bar{\mathbf{B}}_k \mathbf{u}_k, \\ &= e^{(\sum_{i=0}^{k-2} \Delta t_{k-i} \mathbf{A})} \bar{\mathbf{C}}_k \bar{\mathbf{B}}_1 \mathbf{u}_1 + \dots + e^{(\sum_{i=0}^{k-j-1} \Delta t_{k-i} \mathbf{A})} \bar{\mathbf{C}}_k \bar{\mathbf{B}}_j \mathbf{u}_j + \dots + \bar{\mathbf{C}}_k \bar{\mathbf{B}}_k \mathbf{u}_k, \end{aligned} \quad (35)$$

where \mathbf{u}_k is the k -th input of \mathbf{M}_u^τ , *i.e.*, $\mathbf{u}_k = \mathbf{M}_u^\tau[k, :]$, and parameters $\mathbf{B} = \text{Linear}_B(\mathbf{M}_u^\tau)$ and $\mathbf{C} = \text{Linear}_C(\mathbf{M}_u^\tau)$. Thus, $\bar{\mathbf{C}}_k$ can be considered as one query of k -th input \mathbf{u}_k and $\bar{\mathbf{B}}_j$ can be considered as the key of j -th input \mathbf{u}_j . Then, $\bar{\mathbf{C}}_k \bar{\mathbf{B}}_j$ can measure the similarity between \mathbf{u}_k and \mathbf{u}_j , similar to the self-attention mechanism.

According to the above-mentioned proof, we can conclude that parameters \mathbf{B} and \mathbf{C} can measure the similarity between current input to the previous ones and selectively copy the previous input.

B.4 More Details about linear Attention Layer

In standard attention [54], we have N query/key/value tokens $Q_i, K_i, V_i \in \mathbb{R}^d$ for $i = 1, \dots, N$, where N is the sequence length and d is the head dimension. For some similarity metric $\text{Sim}: \mathbb{R}^d \times \mathbb{R}^d \rightarrow \mathbb{R}$, we want to compute the output:

$$O_i = \frac{\sum_{j=1}^i \text{Sim}(Q_i, K_j) V_j}{\sum_{j=1}^i \text{Sim}(Q_i, K_j)} \in \mathbb{R}^d.$$

For standard softmax attention, $\text{Sim}(q, k) = e^{q^\top k}$ (often the dot product is scaled by $1/\sqrt{d}$). Linear attention makes the assumption that Sim has the form $\text{Sim}(q, k) = \phi(q)^\top \phi(k)$, for some (nonlinear) function ϕ . The output is then $O_i = \frac{\phi(Q_i)^\top \sum_{j=1}^i \phi(K_j) V_j^\top}{\phi(Q_i)^\top \sum_{j=1}^i \phi(K_j)}$. Let $S_i = \sum_{j=1}^i \phi(K_j) V_j^\top \in \mathbb{R}^{d \times d}$, $z_i = \sum_{j=1}^i \phi(K_j) \in \mathbb{R}^d$, $d_i = \phi(Q_i)^\top z_i \in \mathbb{R}$. Then $O_i = \frac{\phi(Q_i)^\top S_i}{d_i}$. This connects linear attention to RNNs: the output O_i is a function of S_i and z_i , both of which are incrementally updated (as cumulative sums).

C Time and Memory Complexity Analysis

In our implementation, we have two DyG-Mamba layers and one cross-attention layer. For a batch size of b , a feature dimension of d , an expanded state dimension $2d$, and an SSM dimension d_{ssm} set to 16. High-bandwidth memory (HBM) and SRAM are two important components for GPUs. SRAM has a larger bandwidth, while HBM has a larger memory size. Inspired by Mamba, DyG-Mamba first reads $O(bL(2d) + 2dd_{ssm})$ bytes of memory (Δ, A, B, C) from slow HBM to fast SRAM. Then, DyG-Mamba obtains the discrete \bar{A}, \bar{B} of a size of $(b, L, 2d, d_{ssm})$ in SRAM. Finally, DyG-Mamba performs SSM operations in SRAM and writes the output of a size of $(b, L, 2d)$ back to HBM. This method helps reduce IO operations from $O(bL(2d)N)$ to $O(bL(2d) + 2dd_{ssm})$. The memory complexity is $O(bL(2d) + 2dd_{ssm})$. For the cross-attention layer, following the complexity of linear attention [57], it costs $O(bLd)$ memory. Therefore, the final memory complexity is $O(3bLd + 2dd_{ssm})$. Since d_{ssm} is relatively smaller than bL , we simplify the memory complexity to $O(bLd)$. The time complexity to calculate B, C, Δ is $O(3bL(2d)d_{ssm})$, and the SSM process is $O(bL(2d)d_{ssm})$. Since the linear cross-attention layer cost $O(bLd)$ time, we simplify the overall time complexity as $O(bLdd_{ssm})$. Compared to traditional transformer-based methods, which exhibit quadratic time and memory complexity $O(bL^2d)$, DyG-Mamba is scalable for large sequence lengths.

D Detailed Experimental Settings

D.1 Hardware Specification and Environment

We conduct experiments on an Ubuntu 22.04 LTS server equipped with one Intel(R) Core(TM) i9-10900X CPU @ 3.70GHz with 10 physical cores and NVIDIA RTX A6000 GPUs (48GB). The code is written in Python 3.10 and we use PyTorch 2.1.0 on CUDA 11.8 to train the model. Implementation details could be found at

D.2 Descriptions of Temporal Graph Datasets

We consider a wide set of dynamic graph datasets from diverse domains, including twelve datasets collected by Edgebank [43], which are publicly available¹:

- **Wikipedia** [27] is a bipartite interaction graph that contains the edits on Wikipedia pages over a month. The nodes represent users and pages, and the links denote the editing behaviors with timestamps. Each link is associated with a 172-dimensional Linguistic Inquiry and Word Count (LIWC) feature [42]. This dataset additionally contains dynamic labels that indicate whether users are temporarily banned from editing.
- **Reddit** [27] is bipartite and records the posts of users under subreddits during one month. Users and subreddits are nodes, and links are the timestamped posting requests. Each link has a 172-dimensional LIWC feature. This dataset also includes dynamic labels representing whether users are banned from posting.
- **MOOC** [27] is a bipartite interaction network of online sources, where nodes are students and course content units (e.g., videos and problem sets). Each link denotes a student’s access behavior to a specific content unit and is assigned with a 4-dimensional feature.
- **LastFM** [27] is bipartite and consists of the information about which songs were listened to by which users over one month. Users and songs are nodes, and links denote the listening behaviors of users.
- **Enron** [47] records the email communications between employees of the ENRON energy corporation over three years.
- **Social Evo.** [36] is a mobile phone proximity network that monitors the daily activities of an entire undergraduate dormitory for a period of eight months, where each link has a 2-dimensional feature.
- **UCI** [39] is an online communication network, where nodes are university students and links are messages posted by students.
- **Can. Parl.** [43]: is a dynamic political network documenting the interactions between Canadian Members of Parliaments (MPs) from 2006 to 2019. Each node is one MP representing an electoral district and each edge is formed when two MPs both voted “yes” on a bill. The edge weights specify the number of times that one MP voted “yes” for another MP in a year.
- **US Legis.** [43]: is a senate co-sponsorship graph which documents social interactions between legislators from the US Senate. The edge weights specify the number of times two congress persons have co-sponsored a bill in a given congress.
- **UN Trade** [43]: is a weighted, directed, food and agriculture trading graph between 181 nations and spanning over 30 years. The data was originally collected by the Food and Agriculture Organization of the United Nations. The weight of each edge

¹<https://zenodo.org/records/dynamic-graphs>

Table 6: Statistics of the datasets.

Datasets	Domains	#Nodes	Total Edges	Bipartite	Duration	Unique Steps	Time Granularity
Wikipedia	Social	9,227	157,474	True	1 month	152,757	Unix timestamps
Reddit	Social	10,984	672,447	True	1 month	669,065	Unix timestamps
MOOC	Interaction	7,144	411,749	True	17 months	345,600	Unix timestamps
LastFM	Interaction	1,980	1,293,103	True	1 month	1,283,614	Unix timestamps
Enron	Social	184	125,235	False	3 years	22,632	Unix timestamps
Social Evo.	Proximity	74	2,099,519	False	8 months	565,932	Unix timestamps
UCI	Social	1,899	59,835	False	196 days	58,911	Unix timestamps
Can. Parl.	Politics	734	74,478	False	14 years	14	years
US Legis.	Politics	225	60,396	False	12 congresses	12	congresses
UN Trade	Economics	255	507,497	False	32 years	32	years
UN Vote	Politics	201	1,035,742	False	72 years	72	years
Contact	Proximity	692	2,426,279	False	1 month	8,064	5 minutes

is the sum of all trading goods from one nation to another in a year. The edge weights specify the total sum of normalized agriculture import or export values between two countries.

- **UN Vote** [43]: is a dataset of roll-call votes in the United Nations General Assembly from 1946 to 2020. If two nations both voted "yes" for an item, then the edge weight between them is incremented by one.
- **Contact** [43]: is a dataset that describes the temporal evolution of physical proximity around 700 university students over a four-week period. Each participant is assigned a unique ID, and edges between users indicate that they are within close proximity of each other. The edge weights indicate the physical proximity between the participants.

We show the statistics of the datasets in Table 6, where #Nodes represent the dimensions of the node and the link features. We notice a slight difference between the statistics of the Contact dataset reported in [43] (which has 694 nodes and 2,426,280 links) and our own calculations, although both are calculated based on the released dataset by [43].

D.3 Details about Negative Sampling Strategies

Following [43], we define the training and testing edge sets as E_{train} and E_{test} . We can then divide the edges of a given dynamic graph into three categories: (a) edges that are only seen during training ($E_{\text{train}} \setminus E_{\text{test}}$), (b) edges that are seen during training and reappear during the test ($E_{\text{train}} \cap E_{\text{test}}$), which can be considered as *transductive* edges, and (c) edges that have not been seen during training and appear only during the test ($E_{\text{test}} \setminus E_{\text{train}}$), which can be considered as *inductive* edges.

Random Negative Sampling (rnd). Current evaluation samples negative edges randomly from almost all possible node pairs of the graphs. At each time step, we have a set of positive edges consisting

of source and destination nodes together with edge timestamps and edge features. To generate negative samples, the standard procedure is to keep the timestamps, features, and source nodes of the positive edges, while choosing destination nodes randomly from all nodes.

Historical Negative Sampling (hist). In historical negative sampling (NS), we focus on sampling negative edges from the set of edges that have been observed during previous timestamps but are absent in the current step. The objective of this strategy is to evaluate whether a given method is able to predict in which timestamps an edge would reoccur, rather than, for example, naively predicting it always reoccurs whenever it has been seen once. Therefore, in historical NS, for a given time step t , we sample from the edges $e \in (E_{\text{train}} \cap \bar{E}_t)$. Note that if the number of available historical edges is insufficient to match the number of positive edges, the remaining negative edges are sampled by the random NS strategy.

Inductive Negative Sampling (ind). While in historical NS we focus on observed training edges, in inductive NS, our focus is to evaluate whether a given method can model the recurrence pattern of edges only seen during test time. At test time, after observing the edges that were not seen during training, the model is asked to predict if such edges exist in future steps of the test phase. Therefore, in the inductive NS, we sample from the edges $e \in (E_{\text{test}} \cap \overline{E_{\text{train}} \cap E_t})$ at time step t . As these edges are not observed during training, they are considered as *inductive* edges. Similar to before, if the number of inductive negative edges is not adequate, the remaining negative edges are sampled by the random NS strategy.

D.4 Detailed Model Configurations, Training and Evaluation Process

Model Configurations For all baselines, we follow the configurations as DyGFormer reported [63]. For DyG-Mamba, we list all configurations in Table 7.

Table 7: Configurations

Configuration	Setting
Learning rate	0.0001
Train Epochs	100
Optimizer	Adam
Dimension of time encoding d_T	100
Dimension of co-occurrence d_C	50
Dimension of aligned encoding d	50
Dimension of Δt_i 's encoder $4d$	200
Dimension of output d_{out}	172
Number of Mamba blocks	2
Dimension of SSM d_{SSM}	16
Expanded factor of Mamba	2
Number of Corss-Attention layer	1

Table 8: Sequence Length Settings

Dataset	Sequence Length
Wikipedia	64
Reddit	64
MOOC	256
LastFM	512
Enron	512
Social Evo.	64
UCI	32
Can. Parl.	2048
US Legis.	272
UN Trade	256
UN Vote	128
Contact	32

Then, we perform the grid search to find the optimal sequence length, with a search range spanning from 32 to 2,048 in powers of 2. It is worth noticing that DyG-Mamba can handle nodes with sequence lengths shorter than the defined length. When the sequence length exceeds the specified length, we truncate the sequence and preserve the most recent interactions up to the defined length. Finally, we present the sequence length settings for different datasets in Table 8.

Pre-Analysis Experimental Settings in Figure 1. We run the pre-experiments on a transductive setting with random negative sampling. All experiments use the same batch size of 200 and run five times to calculate the standard deviation. The configurations are chosen by the best performance configuration reported in [63]. The vanilla Mamba is implemented by simply replacing the Transformer layer of DyGFormer with the Mamba layer, and it shares the same configurations as DyGFormer. The ‘without time information’ implementation is achieved by removing the input of time encoding. Since removing the time encoding leaves GraphMixer with no available features for training, we add edge ID information to both the experimental group and the control group. The implementation of “without time information” is achieved by replacing

the timestamps of the temporal sequences with positions, similar to the position encoding in the vanilla Transformer.

Time, Memory comparison Settings in Figure 3 and Figure 4.

In the evaluation of time and memory consumption, we do not choose the configuration as reported in DyGLib², as there is a significant difference in sequence lengths between different baselines. For example, in the LastFM dataset, the reported number of sampled neighbors for DyRep, TGN, and GraphMixer is set to 10, while for DyGFormer and DyG-Mamba, it is 512. This is unfair because the complexity of time and memory is highly dependent on the number of neighbors sampled. Therefore, for a fair comparison in terms of time and memory consumption, we use the same number of sampled neighbors across all models: 32 for UCI, 256 for Enron, 512 for LastFM and 64 for Reddit.

Attention Investigation in Figure 6. We conduct a case study to reveal the attention mapping in DyG-Mamba. We select a pair of nodes (1181, 1173) and sample the neighbors of the source node. In the finely trained model, we extract the output of the readout layer, the last Mamba layer, and the second-last Mamba layer. Then, we calculate the normalized cosine similarity between the target node representation and the last hidden state of the source node to determine whether the model can distinguish the target node. Furthermore, we calculate the similarity between the last hidden states and the second-last hidden states to see whether the model can distinguish the target node during the attention process.

Robustness Test Settings in Figure 8. The purpose of the robustness test is to evaluate the ability to against noise in edges and timestamps. In the training step, we typically train models on a transductive setting with random negative sampling. In the evaluation step, after neighbor sampling, we randomly select $\sigma * L$ positions to insert noise. Specifically, the noise position’s node and timestamps are randomly generated. And the noise rate σ is chosen from 0.1 to 0.6.

E Additional Experimental Results

E.1 Additional Results for Transductive Dynamic Link Prediction

We show the AUC-ROC for transductive dynamic link prediction with three negative sampling strategies in Table 9. Please note that since we cannot reproduce the same performance reported by FreeDyG [51], we directly copy the results from their paper.

E.2 Additional Results for Inductive Dynamic Link Prediction

We present the AP and AUC-ROC for inductive dynamic link prediction with three negative sampling strategies in Table 10 and Table 11.

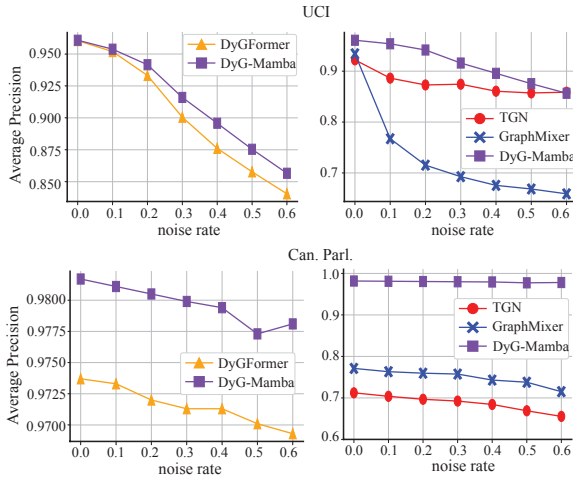
E.3 Additional Results of Robustness test

We present additional results of the robustness test on the UCI and Can. Parl. datasets on Figure 9. From the figure, we can see that our model is consistently more robust than DyGFormer and

²github.com/yule-BUAA/DyGLib

Table 9: AUC-ROC for transductive dynamic link prediction with random, historical, and inductive negative sampling strategies.

NSS	Datasets	JODIE	DyRep	TGAT	TGN	CAWN	EdgeBank	TCL	GraphMixer	FreeDyG	DyGFormer	DyG-Mamba
rand	Wikipedia	96.33 ± 0.07	94.37 ± 0.09	96.67 ± 0.07	98.37 ± 0.07	98.54 ± 0.04	90.78 ± 0.00	95.84 ± 0.18	96.92 ± 0.03	99.41 ± 0.01	98.91 ± 0.02	<u>99.01 ± 0.09</u>
	Reddit	98.31 ± 0.05	98.17 ± 0.05	98.47 ± 0.02	98.60 ± 0.06	99.01 ± 0.01	95.37 ± 0.00	97.42 ± 0.02	97.17 ± 0.02	99.50 ± 0.01	99.15 ± 0.01	<u>99.21 ± 0.00</u>
	MOOC	83.81 ± 2.09	85.03 ± 0.58	87.11 ± 0.19	91.21 ± 1.15	80.38 ± 0.26	60.86 ± 0.00	83.12 ± 0.18	84.01 ± 0.17	89.93 ± 0.35	87.91 ± 0.58	<u>91.01 ± 0.14</u>
	LastFM	70.49 ± 1.66	71.16 ± 1.89	71.59 ± 0.18	78.47 ± 2.94	85.92 ± 0.10	83.77 ± 0.00	64.06 ± 1.16	73.53 ± 0.12	<u>93.42 ± 0.15</u>	93.05 ± 0.10	94.02 ± 0.04
	Enron	87.96 ± 0.52	84.89 ± 3.00	68.89 ± 1.10	88.32 ± 0.99	90.45 ± 0.14	87.05 ± 0.00	75.74 ± 0.72	84.38 ± 0.21	94.01 ± 0.11	<u>93.33 ± 0.13</u>	93.05 ± 0.17
	Social Evo.	92.05 ± 0.46	90.76 ± 0.21	94.76 ± 0.16	95.39 ± 0.17	87.34 ± 0.08	81.60 ± 0.00	94.84 ± 0.17	95.23 ± 0.07	96.59 ± 0.04	96.30 ± 0.01	<u>96.38 ± 0.01</u>
	UCI	90.44 ± 0.49	68.77 ± 2.34	78.53 ± 0.74	92.03 ± 1.13	93.87 ± 0.08	77.30 ± 0.00	87.82 ± 1.36	91.81 ± 0.67	<u>95.00 ± 0.21</u>	94.49 ± 0.26	95.32 ± 0.18
	Can. Parl.	78.21 ± 0.23	73.35 ± 3.67	75.69 ± 0.78	76.99 ± 1.80	75.70 ± 3.27	64.14 ± 0.00	72.46 ± 3.23	83.17 ± 0.53	N/A	<u>97.76 ± 0.41</u>	98.67 ± 0.29
	US Legis.	82.85 ± 1.07	82.68 ± 0.32	75.84 ± 1.99	83.34 ± 0.43	77.16 ± 0.39	62.57 ± 0.00	76.27 ± 0.63	76.96 ± 0.79	N/A	77.90 ± 0.58	78.19 ± 0.64
	UN Trade	69.62 ± 0.44	67.44 ± 0.83	64.01 ± 0.12	69.10 ± 1.67	68.54 ± 0.18	66.75 ± 0.00	64.72 ± 0.05	65.52 ± 0.51	N/A	<u>70.20 ± 1.44</u>	72.19 ± 0.09
	UN Vote	68.53 ± 0.95	67.18 ± 1.04	52.83 ± 1.12	69.71 ± 2.65	53.09 ± 0.22	62.97 ± 0.00	51.88 ± 0.36	52.46 ± 0.27	N/A	57.12 ± 0.62	68.46 ± 1.64
	Contact	96.66 ± 0.89	96.48 ± 0.14	96.95 ± 0.08	97.54 ± 0.35	89.99 ± 0.34	94.34 ± 0.00	94.15 ± 0.09	93.94 ± 0.02	N/A	98.53 ± 0.01	98.59 ± 0.00
	Avg. Rank		5.25	6.75	7.00	3.25	5.58	8.17	8.25	6.58	N/A	<u>2.58</u>
hist	Wikipedia	80.77 ± 0.73	77.74 ± 0.33	82.87 ± 0.22	82.74 ± 0.32	67.84 ± 0.64	77.27 ± 0.00	85.76 ± 0.46	87.68 ± 0.17	82.78 ± 0.30	78.80 ± 1.95	79.12 ± 1.38
	Reddit	80.52 ± 0.32	80.15 ± 0.18	79.33 ± 0.16	81.11 ± 0.19	80.27 ± 0.30	78.58 ± 0.00	76.49 ± 0.16	77.80 ± 0.12	85.92 ± 0.10	80.54 ± 0.29	80.89 ± 0.20
	MOOC	82.75 ± 0.83	81.06 ± 0.94	80.81 ± 0.67	88.00 ± 1.80	71.57 ± 1.07	61.90 ± 0.00	72.09 ± 0.56	76.68 ± 1.40	<u>88.32 ± 0.99</u>	87.04 ± 0.35	88.72 ± 1.03
	LastFM	75.22 ± 2.36	74.65 ± 1.98	64.27 ± 0.26	77.97 ± 3.04	67.88 ± 0.24	78.09 ± 0.00	47.24 ± 3.13	64.21 ± 0.12	73.53 ± 0.12	<u>78.78 ± 0.35</u>	80.85 ± 0.52
	Enron	75.39 ± 2.37	74.69 ± 3.55	61.85 ± 1.43	77.09 ± 2.22	65.10 ± 0.34	79.59 ± 0.00	67.95 ± 0.88	75.27 ± 1.14	75.74 ± 0.72	76.55 ± 0.52	<u>78.17 ± 0.64</u>
	Social Evo.	90.06 ± 3.15	93.12 ± 0.34	93.08 ± 0.59	94.71 ± 0.53	87.43 ± 0.15	85.81 ± 0.00	93.44 ± 0.68	94.39 ± 0.31	97.42 ± 0.02	97.28 ± 0.07	<u>97.35 ± 0.08</u>
	UCI	78.64 ± 3.50	57.91 ± 3.12	58.89 ± 1.57	77.25 ± 2.68	57.86 ± 0.15	69.56 ± 0.00	72.25 ± 3.46	77.54 ± 2.02	80.38 ± 0.26	76.97 ± 0.24	76.70 ± 0.25
	Can. Parl.	62.44 ± 1.11	70.16 ± 1.70	70.86 ± 0.94	73.23 ± 3.08	72.06 ± 3.94	63.04 ± 0.00	69.95 ± 3.70	79.03 ± 1.01	N/A	97.61 ± 0.40	<u>96.97 ± 0.30</u>
	US Legis.	67.47 ± 6.40	91.44 ± 1.18	73.47 ± 5.25	83.53 ± 4.53	78.62 ± 7.46	67.41 ± 0.00	83.97 ± 3.71	85.17 ± 0.70	N/A	90.77 ± 1.96	92.70 ± 0.30
	UN Trade	68.92 ± 1.40	64.36 ± 1.40	60.37 ± 0.68	63.93 ± 5.41	63.09 ± 0.74	86.61 ± 0.00	61.43 ± 1.04	63.20 ± 1.54	N/A	73.86 ± 1.13	<u>75.11 ± 0.16</u>
	UN Vote	76.84 ± 1.01	74.72 ± 1.43	53.95 ± 3.15	73.40 ± 5.20	51.27 ± 0.33	89.62 ± 0.00	52.29 ± 2.39	52.61 ± 1.44	N/A	64.27 ± 1.78	65.16 ± 4.43
	Contact	96.35 ± 0.92	96.00 ± 0.23	95.39 ± 0.43	93.76 ± 1.29	83.06 ± 0.32	92.17 ± 0.00	93.34 ± 0.19	93.14 ± 0.34	N/A	<u>97.17 ± 0.05</u>	97.35 ± 0.01
	Avg. Rank		5.00	5.67	7.08	3.83	8.25	6.50	7.25	5.67	N/A	<u>3.33</u>
ind	Wikipedia	70.96 ± 0.78	67.36 ± 0.96	81.93 ± 0.22	80.97 ± 0.31	70.95 ± 0.95	81.73 ± 0.00	82.19 ± 0.48	84.28 ± 0.30	<u>82.74 ± 0.32</u>	75.09 ± 3.70	82.30 ± 1.81
	Reddit	83.51 ± 0.15	82.90 ± 0.31	87.13 ± 0.20	84.56 ± 0.24	88.04 ± 0.29	85.93 ± 0.00	84.67 ± 0.29	82.21 ± 0.13	84.38 ± 0.21	86.23 ± 0.51	86.99 ± 0.55
	MOOC	66.63 ± 2.30	63.26 ± 1.01	73.18 ± 0.33	77.44 ± 2.86	70.32 ± 1.43	48.18 ± 0.00	70.36 ± 0.37	72.45 ± 0.72	78.47 ± 0.94	<u>80.76 ± 0.76</u>	82.05 ± 1.38
	LastFM	61.32 ± 3.49	62.15 ± 2.12	63.99 ± 0.21	65.46 ± 4.27	67.92 ± 0.44	77.37 ± 0.00	46.93 ± 2.59	60.22 ± 0.32	<u>72.30 ± 0.59</u>	69.25 ± 0.36	69.13 ± 0.59
	Enron	70.92 ± 1.05	68.73 ± 1.34	60.45 ± 2.12	71.34 ± 2.46	<u>75.17 ± 0.50</u>	75.00 ± 0.00	67.64 ± 0.86	71.53 ± 0.85	77.27 ± 0.61	74.07 ± 0.64	74.49 ± 0.48
	Social Evo.	90.01 ± 3.19	93.07 ± 0.38	92.94 ± 0.61	95.24 ± 0.56	89.93 ± 0.15	87.88 ± 0.00	93.44 ± 0.72	94.22 ± 0.32	98.47 ± 0.02	97.51 ± 0.06	<u>97.64 ± 0.07</u>
	UCI	64.14 ± 1.26	54.25 ± 2.01	60.80 ± 1.01	64.11 ± 1.04	58.06 ± 0.26	58.03 ± 0.00	70.05 ± 1.86	<u>74.59 ± 0.74</u>	75.39 ± 0.57	65.96 ± 1.18	73.23 ± 1.03
	Can. Parl.	52.88 ± 0.80	63.53 ± 0.65	72.47 ± 1.18	69.57 ± 2.81	72.93 ± 1.78	61.41 ± 0.00	69.47 ± 2.12	70.52 ± 0.94	N/A	<u>96.70 ± 0.59</u>	97.30 ± 0.97
	US Legis.	59.05 ± 5.52	89.44 ± 0.71	71.62 ± 5.42	78.12 ± 4.46	76.45 ± 7.02	68.66 ± 0.00	82.54 ± 3.91	84.22 ± 0.91	N/A	87.96 ± 1.80	90.28 ± 0.50
	UN Trade	66.82 ± 1.27	65.60 ± 1.28	66.13 ± 0.78	66.37 ± 5.39	<u>71.73 ± 0.74</u>	74.20 ± 0.00	67.80 ± 1.21	66.53 ± 1.22	N/A	62.56 ± 1.51	69.09 ± 1.28
	UN Vote	73.73 ± 1.61	72.80 ± 2.16	53.04 ± 2.58	72.69 ± 3.72	52.75 ± 0.90	<u>72.85 ± 0.00</u>	52.02 ± 1.64	51.89 ± 0.74	N/A	53.37 ± 1.26	63.69 ± 3.97
	Contact	94.47 ± 1.08	94.23 ± 0.18	94.10 ± 0.41	91.64 ± 1.72	87.68 ± 0.24	85.87 ± 0.00	91.23 ± 0.19	90.96 ± 0.27	N/A	<u>95.01 ± 0.15</u>	95.08 ± 0.01
	Avg. Rank		6.75	7.08	6.00	5.42	5.67	6.08	6.17	5.67	N/A	<u>4.00</u>

**Figure 9: The robustness test on datasets UCI, Can. Parl. with the noise ratio from 0.1 to 0.6.**

GraphMixer. However, TGN has a memory bank to remember all the node representations in the past, so adding noise to the current neighbors has less effect on its performance.

E.4 Results of Training Time and Parameter Size Comparisons

Figure 10 shows the additional time and parameter size comparison on the UCI, Enron, LastFM, and Reddit datasets. The models that do not appear in the figure experienced out-of-memory (OOM) errors. We can see that our model achieves the best performance while incurring relatively low time and memory costs.

E.5 Results of Ablation Study

We validate the effectiveness of several designs in DyG-Mamba via an ablation study, including the selective mechanism in Mamba, the use of continuous SSM, and the use of a cross-attention layer. We, respectively, remove these modules and denote the remaining parts as w/o Selective, w/o Time-Span, and w/o Cross-attn. We report the performance of different variants on Can. Parl. and Enron in Figure 5, UCI, and UNLegis at Figure 11.

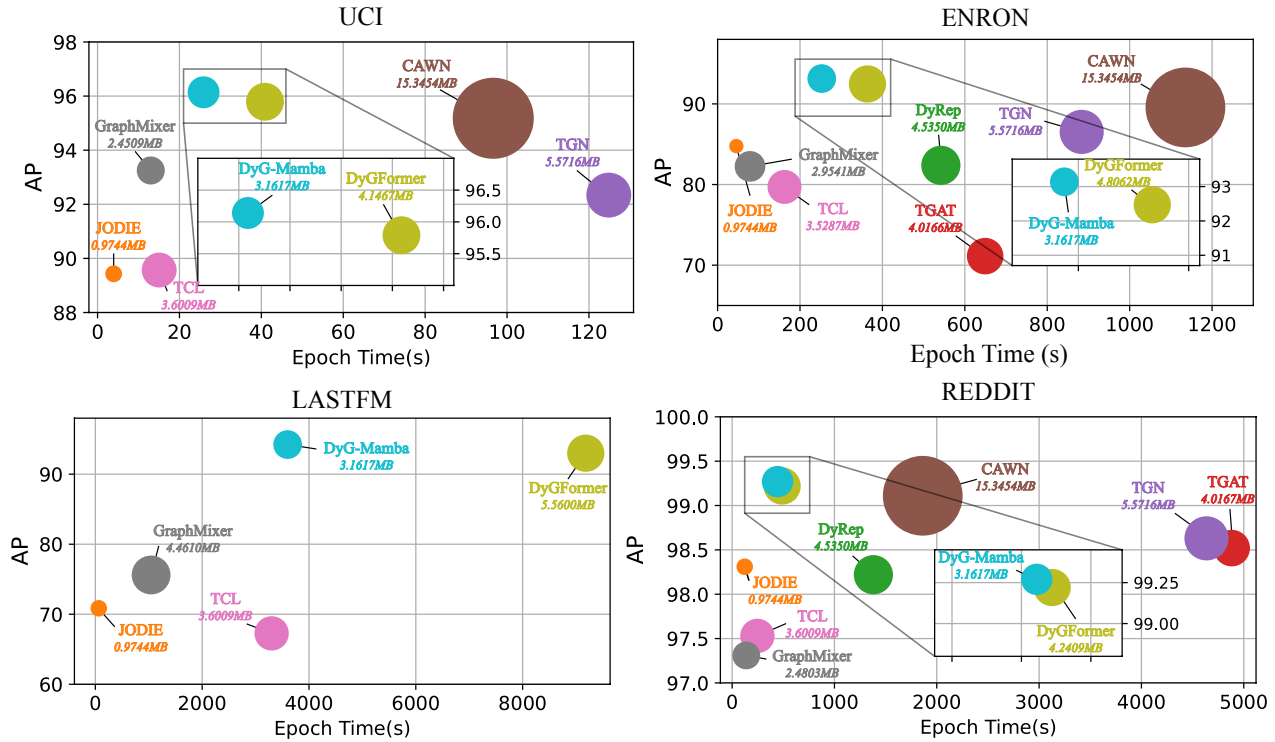


Figure 10: The AP score with different sequence lengths. We use the same sequence length for each model (uci=32, enron=256, lastfm=512, reddit=64), The not appearing model means OOM.

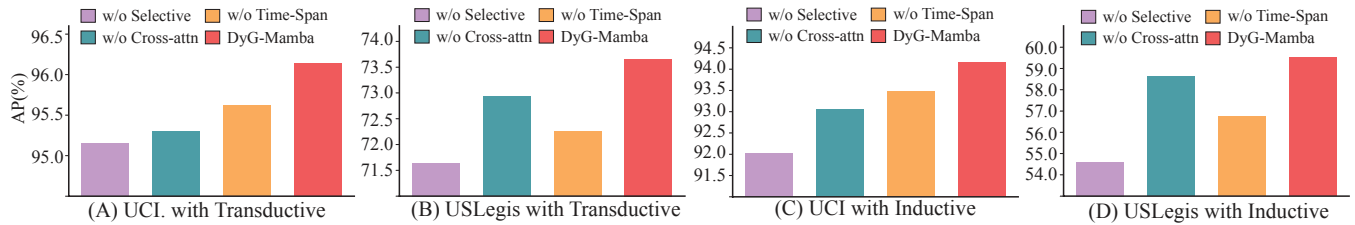


Figure 11: Ablation study of the components in DyG-Mamba on datasets UCI and USLegis.

Our findings from Figure 5 and Figure 11 indicate that DyG-Mamba achieves optimal performance when all components are utilized. The removal of any component would lead to worse results. In particular, the performance of the model without time-span decreases significantly, especially in inductive settings, demonstrating the effectiveness of time-span as a control signal. Secondly, performance also decreases without selective updating because the fixed update mode cannot adapt to dynamic networks. The cross-attention between the source node and destination node results in relatively minor improvements due to the use of neighbor co-occurrence encoding, which also explores the mutual information between the two sequences. Thus, the necessity of designing these components has been well demonstrated.

F Limitations

Although we achieve good performance on dynamic graph learning, we still have several limitations. (i) In this paper, we focus mainly on link addition, which is a widely studied interaction type in previous research. We leave the investigations of other interaction types (e.g., node addition/deletion/feature transformations and link deletion/feature transformations) for future work. (ii) In this paper, the scale of the dataset is limited and the results for larger or more real-world applications are still unknown. (iii) Although DyG-Mamba has achieved good results in dynamic network learning, it is still unknown whether this conclusion can be extended to other fields, especially recently when Mambaout [64] suggests that Mamba is more suitable for auto-regressive and long sequence tasks. Although dynamic link prediction and node classification

tasks are not auto-regressive tasks, we can still achieve state-of-the-art results, indicating that the effectiveness of Mamba in different tasks is still worth further exploration.

G Impact Statements

In this section, we elaborate on the broader impacts of our work from the following two aspects. (i) *Dynamic graph learning*: With the rapid development of social networks and economic networks, dynamic graph learning has become a significant research topic in the machine learning community. Compared to current dynamic graph learning methods, our work introduces a new Mamba-based dynamic graph learning framework. Additionally, we incorporate irregular time-spans as control signals for SSM, enhancing the model's time-awareness. (ii) *Time Information Effects*: Despite significant advances in dynamic graph learning, there is still a lack of theoretical foundations regarding the time information between the evolution laws of dynamic graphs. Our work highlights the significant potential of a time-span-based memory updating mechanism in dynamic graph learning, which may assist others in comprehending the time theory. Moreover, we do not anticipate any direct negative impacts on society from our findings.

H Algorithm

In this section, we list the Continuous SSM procedure in [Algorithm. 1](#), the procedures of downstream tasks link prediction on [Algorithm. 2](#), node classification on [Algorithm. 3](#).

Algorithm 1: Continuous SSM

Input : Hidden states $Z = \{z_{i,1}, z_{i,2}, \dots, z_{i,L}\}_{i=1}^B$: (B, L, d) , Control signals $\Delta t = \{\Delta t_1, \Delta t_2, \dots, \Delta t_L\}$: (B, L, d) , SSM dimension d_{ssm} , Expanded dimension: $2d$.

Output : Updated hidden states \hat{Z} : $(B, L, 2d)$.

```

1 // Normalize the input sequence.
2 initialize  $\mathbf{Parameter}_i^A: (2d, d_{ssm})$ ,  $\mathbf{Parameter}_i^{\Delta}: (d_{ssm})$ 
3  $Z'$ :  $(B, L, d) \leftarrow \mathbf{Norm}(Z)$ 
4  $x$ :  $(B, L, 2d) \leftarrow \mathbf{Linear}^x(Z)$ 
5  $z$ :  $(B, L, 2d) \leftarrow \mathbf{Linear}^z(Z)$ 
6  $\Delta t$ :  $(B, L, 2d) \leftarrow \mathbf{Linear}^{\Delta t}(\Delta t)$ 
7 for  $o$  in {forward, backward} do
8    $x'_o$ :  $(B, L, 2d) \leftarrow \mathbf{SiLU}(\mathbf{Conv1d}_o(x))$ 
9    $B_o$ :  $(B, L, d_{ssm}) \leftarrow \mathbf{Linear}_o^B(x'_o)$ 
10   $C_o$ :  $(B, L, d_{ssm}) \leftarrow \mathbf{Linear}_o^C(x'_o)$ 
11  // Control signal to control the selection of historical information.
12   $\Delta_o$ :  $(B, L, 2d) \leftarrow \log(1 + \exp(\mathbf{Linear}_o^{\Delta}(\Delta t'_o) + \mathbf{Parameter}_o^{\Delta}))$  // softplus.
13   $\bar{A}_o$ :  $(B, L, 2d, d_{ssm}) \leftarrow \Delta_i \otimes \mathbf{Parameter}_o^A$ 
14   $\bar{B}_o$ :  $(B, L, 2d, d_{ssm}) \leftarrow \Delta_i \otimes B_o$ 
15   $y_o$ :  $(B, L, 2d) \leftarrow \mathbf{SSM}(\bar{A}_o, \bar{B}_o, C_o)(x'_o)$ 
16 end
17 // Gated  $y$ .
18  $y'_{forward}$ :  $(B, L, 2d) \leftarrow y_{forward} \odot \mathbf{SiLU}(z)$ 
19  $y'_{backward}$ :  $(B, L, 2d) \leftarrow y_{backward} \odot \mathbf{SiLU}(z)$  // Residual connection.
20  $\hat{Z}$ :  $(B, L, d) \leftarrow \mathbf{Linear}^T(y'_{forward} + y'_{backward}) + Z$ 
21 Return  $\hat{Z}$ 

```

Algorithm 2: Dynamic Link Prediction

Input : The dynamic interaction set $\mathcal{D} = \{(u_i, v_i, t_i)\}_{i=1}^K$, Continuous SSM $CSSM(\cdot)$, cross-attention layer $CrossAttn(\cdot)$, readout function $r(\cdot)$, output projection layer $\phi(\cdot)$.

```

1 for  $T$  Epochs do
2   for  $(u_1, u_2, t) \in \mathcal{D}$  do
3     For a node pair  $(u_1, u_2)$ . Sampled neighbor sequence:  $S_1, S_2$ .
4     for  $u$  in  $\{u_1, u_2\}$  do
5       Node Features:  $\mathbf{v}_{u,k_i} \in \mathbb{R}^{d_v}$ , Edge Features:  $\mathbf{e}_{u,k_i} \in \mathbb{R}^{d_E}$ ,
6       Time Features:  $\mathbf{t}_{u,k_i} \in \mathbb{R}^{d_T}$ , Co-occurrence Features:  $\mathbf{c}_{u,k_i} \in \mathbb{R}^{d_C}$ ,
7       Time Span:  $\Delta t_u = \{\Delta t_1, \Delta t_2, \dots, \Delta t_L\}$ 
8       // Feature Alignment.
9        $\mathbf{Z}_{u,*} = \mathbf{X}_{u,*} \mathbf{W}_* + \mathbf{b}$ , where  $*$   $\in N, E, T, C$ 
10       $\mathbf{Z}_u = \mathbf{Z}_{u,N} \parallel \mathbf{Z}_{u,E} \parallel \mathbf{Z}_{u,T} \parallel \mathbf{Z}_{u,C}$ 
11      // Continuous SSM encoder.
12       $\hat{\mathbf{Z}}_u = CSSM(\mathbf{Z}_u, \Delta t_u)$ 
13    end
14    Compute the Cross Attention,  $\mathbf{H}_{u_1}$  and  $\mathbf{H}_{u_2}$  between two sequences as Eqs.(10, 11, 12, 13).
15     $\mathbf{h}_{u_1} = \phi(r(\mathbf{H}_{u_1}))$ ,  $\mathbf{h}_{u_2} = \phi(r(\mathbf{H}_{u_2}))$ . // Output.
16     $\hat{y} = \text{Softmax}(\text{Linear}(\text{RELU}(\text{Linear}(\mathbf{h}_{u_1}^T \parallel \mathbf{h}_{u_2}^T))))$ .
17  end
18  Compute  $\mathcal{L}_{\text{Link Prediction}}$ .
19 end

```

Algorithm 3: Dynamic Node Classification

Input : The dynamic interaction set $\mathcal{D} = \{(u_i, y_i)\}_{i=1}^N$, Continuous SSM $CSSM(\cdot)$, readout function $r(\cdot)$, output projection layer $\phi(\cdot)$.

```

1 for  $T$  Epochs do
2   for  $(u, y) \in \mathcal{D}$  do
3     Sampled neighbor sequence:  $S = \{(k_1, t_1), (k_2, t_2), \dots, (k_L, t_L)\}$ ,
4     Node Features:  $\mathbf{v}_{u,k_i} \in \mathbb{R}^{d_v}$ , Edge Features:  $\mathbf{e}_{u,k_i} \in \mathbb{R}^{d_E}$ ,
5     Time Features:  $\mathbf{t}_{u,k_i} \in \mathbb{R}^{d_T}$ , Time Span:  $\Delta t_u = \{\Delta t_1, \Delta t_2, \dots, \Delta t_L\}$   $\mathbf{Z}_{u,*} = \mathbf{X}_{u,*} \mathbf{W}_* + \mathbf{b}$ , where  $*$   $\in N, E, T$ .
6      $\mathbf{Z}_u = \mathbf{Z}_{u,N} \parallel \mathbf{Z}_{u,E} \parallel \mathbf{Z}_{u,T}$   $\hat{\mathbf{H}}_u = CSSM(\mathbf{Z}_u, \Delta t_u)$   $\mathbf{h}_u = \phi(r(\mathbf{H}_u))$   $\hat{y} = \text{Softmax}(\text{Linear}(\text{RELU}(\text{Linear}(\mathbf{h}_u^T))))$ .
7   end
8   Compute  $\mathcal{L}_{\text{Node Classification}}$ .
9 end

```

Table 10: AP for inductive dynamic link prediction with random, historical, and inductive negative sampling strategies.

NSS	Datasets	JODIE	DyRep	TGAT	TGN	CAWN	TCL	GraphMixer	FreeDyG	DyGFormer	DyG-Mamba
rnd	Wikipedia	94.82 ± 0.20	92.43 ± 0.37	96.22 ± 0.07	97.83 ± 0.04	98.24 ± 0.03	96.22 ± 0.17	96.65 ± 0.02	98.97 ± 0.01	98.59 ± 0.03	<u>98.65 ± 0.03</u>
	Reddit	96.50 ± 0.13	96.09 ± 0.11	97.09 ± 0.04	97.50 ± 0.07	98.62 ± 0.01	94.09 ± 0.07	95.26 ± 0.02	98.91 ± 0.01	98.84 ± 0.02	<u>98.88 ± 0.00</u>
	MOOC	79.63 ± 1.92	81.07 ± 0.44	85.50 ± 0.19	<u>89.04 ± 1.17</u>	81.42 ± 0.24	80.60 ± 0.22	81.41 ± 0.21	87.75 ± 0.62	86.96 ± 0.43	90.20 ± 0.06
	LastFM	81.61 ± 3.82	83.02 ± 1.48	78.63 ± 0.31	81.45 ± 4.29	89.42 ± 0.07	73.53 ± 1.66	82.11 ± 0.42	<u>94.89 ± 0.01</u>	94.23 ± 0.09	95.13 ± 0.08
	Enron	80.72 ± 1.39	74.55 ± 3.95	67.05 ± 1.51	77.94 ± 1.02	86.35 ± 0.51	76.14 ± 0.79	75.88 ± 0.48	89.69 ± 0.17	<u>89.76 ± 0.34</u>	91.14 ± 0.07
	Social Evo.	91.96 ± 0.48	90.04 ± 0.47	91.41 ± 0.16	90.77 ± 0.86	79.94 ± 0.18	91.55 ± 0.09	91.86 ± 0.06	94.76 ± 0.05	93.14 ± 0.04	<u>93.23 ± 0.01</u>
	UCI	79.86 ± 1.48	57.48 ± 1.87	79.54 ± 0.48	88.12 ± 2.05	92.73 ± 0.06	87.36 ± 2.03	91.19 ± 0.42	94.85 ± 0.10	<u>94.54 ± 0.12</u>	94.15 ± 0.04
	Can. Parl.	53.92 ± 0.94	54.02 ± 0.76	55.18 ± 0.79	54.10 ± 0.93	55.80 ± 0.69	54.30 ± 0.66	55.91 ± 0.82	N/A	<u>87.74 ± 0.71</u>	90.05 ± 0.86
	US Legis.	54.93 ± 2.29	57.28 ± 0.71	51.00 ± 3.11	<u>58.63 ± 0.37</u>	53.17 ± 1.20	52.59 ± 0.97	50.71 ± 0.76	N/A	54.28 ± 2.87	59.52 ± 0.54
	UN Trade	59.65 ± 0.77	57.02 ± 0.69	61.03 ± 0.18	58.31 ± 3.15	<u>65.24 ± 0.21</u>	62.21 ± 0.12	62.17 ± 0.31	N/A	64.55 ± 0.62	65.87 ± 0.40
	UN Vote	56.64 ± 0.96	54.62 ± 2.22	52.24 ± 1.46	<u>58.85 ± 2.51</u>	49.94 ± 0.45	51.60 ± 0.97	50.68 ± 0.44	N/A	55.93 ± 0.39	59.89 ± 1.04
	Contact	94.34 ± 1.45	92.18 ± 0.41	95.87 ± 0.11	93.82 ± 0.99	89.55 ± 0.30	91.11 ± 0.12	90.59 ± 0.05	N/A	<u>98.03 ± 0.02</u>	98.12 ± 0.04
Avg. Rank	5.83	6.92	6.21	4.83	4.92	6.71	6.00	N/A	2.50	1.08	
hist	Wikipedia	68.69 ± 0.39	62.18 ± 1.27	<u>84.17 ± 0.22</u>	81.76 ± 0.32	67.27 ± 1.63	82.20 ± 2.18	87.60 ± 0.30	82.78 ± 0.30	71.42 ± 4.43	79.50 ± 2.77
	Reddit	62.34 ± 0.54	61.60 ± 0.72	63.47 ± 0.36	64.85 ± 0.85	63.67 ± 0.41	60.83 ± 0.25	64.50 ± 0.26	66.02 ± 0.41	65.37 ± 0.60	<u>65.65 ± 0.00</u>
	MOOC	63.22 ± 1.55	62.93 ± 1.24	76.73 ± 0.29	77.07 ± 3.41	74.68 ± 0.68	74.27 ± 0.53	74.00 ± 0.97	<u>81.63 ± 0.33</u>	80.82 ± 0.30	81.66 ± 1.09
	LastFM	70.39 ± 4.31	71.45 ± 1.76	76.27 ± 0.25	66.65 ± 6.11	71.33 ± 0.47	65.78 ± 0.65	76.42 ± 0.22	<u>77.28 ± 0.21</u>	76.35 ± 0.52	79.60 ± 0.28
	Enron	65.86 ± 3.71	62.08 ± 2.27	61.40 ± 1.31	62.91 ± 1.16	60.70 ± 0.36	67.11 ± 0.62	<u>72.37 ± 1.37</u>	73.01 ± 0.88	67.07 ± 0.62	68.44 ± 1.85
	Social Evo.	88.51 ± 0.87	88.72 ± 1.10	93.97 ± 0.54	90.66 ± 1.62	79.83 ± 0.38	94.10 ± 0.31	94.01 ± 0.47	96.69 ± 0.14	<u>96.82 ± 0.16</u>	96.92 ± 0.22
	UCI	63.11 ± 2.27	52.47 ± 2.06	70.52 ± 0.93	70.78 ± 0.78	64.54 ± 0.47	76.71 ± 1.00	<u>81.66 ± 0.49</u>	82.35 ± 0.39	72.13 ± 1.87	79.30 ± 1.02
	Can. Parl.	52.60 ± 0.88	52.28 ± 0.31	56.72 ± 0.47	54.42 ± 0.77	57.14 ± 0.07	55.71 ± 0.74	55.84 ± 0.73	N/A	<u>87.40 ± 0.85</u>	89.42 ± 0.38
	US Legis.	52.94 ± 2.11	<u>62.10 ± 1.41</u>	51.83 ± 3.95	61.18 ± 1.10	55.56 ± 1.71	53.87 ± 1.41	52.03 ± 1.02	N/A	56.31 ± 3.46	64.23 ± 0.11
	UN Trade	55.46 ± 1.19	<u>55.49 ± 0.84</u>	55.28 ± 0.71	52.80 ± 3.19	55.00 ± 0.38	55.76 ± 1.03	54.94 ± 0.97	N/A	53.20 ± 1.07	54.62 ± 0.19
	UN Vote	<u>61.04 ± 1.30</u>	60.22 ± 1.78	53.05 ± 3.10	63.74 ± 3.00	47.98 ± 0.84	54.19 ± 2.17	48.09 ± 0.43	N/A	52.63 ± 1.26	58.61 ± 0.04
	Contact	90.42 ± 2.34	89.22 ± 0.66	94.15 ± 0.45	88.13 ± 1.50	74.20 ± 0.80	90.44 ± 0.17	89.91 ± 0.36	N/A	93.56 ± 0.52	<u>93.65 ± 0.20</u>
Avg. Rank	6.25	6.42	4.92	5.25	6.67	4.83	4.42	N/A	3.92	2.33	
ind	Wikipedia	68.70 ± 0.39	62.19 ± 1.28	84.17 ± 0.22	81.77 ± 0.32	67.24 ± 1.63	82.20 ± 2.18	87.60 ± 0.29	<u>87.54 ± 0.26</u>	71.42 ± 4.43	79.44 ± 2.78
	Reddit	62.32 ± 0.54	61.58 ± 0.72	63.40 ± 0.36	64.84 ± 0.84	63.65 ± 0.41	60.81 ± 0.26	64.49 ± 0.25	64.98 ± 0.20	<u>65.35 ± 0.60</u>	65.61 ± 0.01
	MOOC	63.22 ± 1.55	62.92 ± 1.24	76.72 ± 0.30	77.07 ± 3.40	74.69 ± 0.68	74.28 ± 0.53	73.99 ± 0.97	<u>81.41 ± 0.31</u>	80.82 ± 0.30	81.67 ± 1.08
	LastFM	70.39 ± 4.31	71.45 ± 1.75	76.28 ± 0.25	69.46 ± 4.65	71.33 ± 0.47	65.78 ± 0.65	76.42 ± 0.22	<u>77.01 ± 0.43</u>	76.35 ± 0.52	79.60 ± 0.28
	Enron	65.86 ± 3.71	62.08 ± 2.27	61.40 ± 1.30	62.90 ± 1.16	60.72 ± 0.36	67.11 ± 0.62	<u>72.37 ± 1.38</u>	72.85 ± 0.81	67.07 ± 0.62	68.44 ± 1.85
	Social Evo.	88.51 ± 0.87	88.72 ± 1.10	93.97 ± 0.54	90.65 ± 1.62	79.83 ± 0.39	94.10 ± 0.32	94.01 ± 0.47	<u>96.91 ± 0.12</u>	96.82 ± 0.17	96.93 ± 0.21
	UCI	63.16 ± 2.27	52.47 ± 2.09	70.49 ± 0.93	70.73 ± 0.79	64.54 ± 0.47	76.65 ± 0.99	<u>81.64 ± 0.49</u>	82.06 ± 0.58	72.13 ± 1.86	79.27 ± 1.03
	Can. Parl.	52.58 ± 0.86	52.24 ± 0.28	56.46 ± 0.50	54.18 ± 0.73	57.06 ± 0.08	55.46 ± 0.69	55.76 ± 0.65	N/A	<u>87.22 ± 0.82</u>	89.04 ± 0.34
	US Legis.	52.94 ± 2.11	<u>62.10 ± 1.41</u>	51.83 ± 3.95	61.18 ± 1.10	55.56 ± 1.71	53.87 ± 1.41	52.03 ± 1.02	N/A	56.31 ± 3.46	64.23 ± 0.11
	UN Trade	55.43 ± 1.20	55.42 ± 0.87	<u>55.58 ± 0.68</u>	52.80 ± 3.24	54.97 ± 0.38	55.66 ± 0.98	54.88 ± 1.01	N/A	52.56 ± 1.70	54.58 ± 0.19
	UN Vote	<u>61.17 ± 1.33</u>	60.29 ± 1.79	53.08 ± 3.10	63.71 ± 2.97	48.01 ± 0.82	54.13 ± 2.16	48.10 ± 0.40	N/A	52.61 ± 1.25	58.66 ± 0.03
	Contact	90.43 ± 2.33	89.22 ± 0.65	94.14 ± 0.45	88.12 ± 1.50	74.19 ± 0.81	90.43 ± 0.17	89.91 ± 0.36	N/A	93.55 ± 0.52	<u>93.64 ± 0.20</u>
Avg. Rank	6.21	6.58	4.75	5.17	6.67	4.88	4.42	N/A	4.00	2.33	

Table 11: AUC-ROC for inductive dynamic link prediction with random, historical, and inductive negative sampling strategies.

NSS	Datasets	JODIE	DyRep	TGAT	TGN	CAWN	TCL	GraphMixer	FreeDyG	DyGFormer	DyG-Mamba
rnd	Wikipedia	94.33 ± 0.27	91.49 ± 0.45	95.90 ± 0.09	97.72 ± 0.03	98.03 ± 0.04	95.57 ± 0.20	96.30 ± 0.04	99.01 ± 0.02	98.48 ± 0.03	<u>98.57 ± 0.08</u>
	Reddit	96.52 ± 0.13	96.05 ± 0.12	96.98 ± 0.04	97.39 ± 0.07	98.42 ± 0.02	93.80 ± 0.07	94.97 ± 0.05	98.84 ± 0.01	98.71 ± 0.01	<u>98.78 ± 0.01</u>
	MOOC	83.16 ± 1.30	84.03 ± 0.49	86.84 ± 0.17	91.24 ± 0.99	81.86 ± 0.25	81.43 ± 0.19	82.77 ± 0.24	87.01 ± 0.74	87.62 ± 0.51	<u>91.05 ± 0.02</u>
	LastFM	81.13 ± 3.39	82.24 ± 1.51	76.99 ± 0.29	82.61 ± 3.15	87.82 ± 0.12	70.84 ± 0.85	80.37 ± 0.18	<u>94.32 ± 0.03</u>	94.08 ± 0.08	94.83 ± 0.01
	Enron	81.96 ± 1.34	76.34 ± 4.20	64.63 ± 1.74	78.83 ± 1.11	87.02 ± 0.50	72.33 ± 0.99	76.51 ± 0.71	89.51 ± 0.20	<u>90.69 ± 0.26</u>	90.84 ± 0.18
	Social Evo.	93.70 ± 0.29	91.18 ± 0.49	93.41 ± 0.19	93.43 ± 0.59	84.73 ± 0.27	93.71 ± 0.18	94.09 ± 0.07	96.41 ± 0.07	95.29 ± 0.03	<u>95.41 ± 0.00</u>
	UCI	78.80 ± 0.94	58.08 ± 1.81	77.64 ± 0.38	86.68 ± 2.29	90.40 ± 0.11	84.49 ± 1.82	89.30 ± 0.57	93.01 ± 0.08	<u>92.63 ± 0.13</u>	91.99 ± 0.03
	Can. Parl.	53.81 ± 1.14	55.27 ± 0.49	56.51 ± 0.75	55.86 ± 0.75	58.83 ± 1.13	55.83 ± 1.07	58.32 ± 1.08	N/A	<u>89.33 ± 0.48</u>	90.77 ± 0.86
	US Legis.	58.12 ± 2.35	<u>61.07 ± 0.56</u>	48.27 ± 3.50	62.38 ± 0.48	51.49 ± 1.13	50.43 ± 1.48	47.20 ± 0.89	N/A	53.21 ± 3.04	56.56 ± 1.08
	UN Trade	62.28 ± 0.50	58.82 ± 0.98	62.72 ± 0.12	59.99 ± 3.50	67.05 ± 0.21	63.76 ± 0.07	63.48 ± 0.37	N/A	<u>67.25 ± 1.05</u>	69.22 ± 0.52
	UN Vote	58.13 ± 1.43	55.13 ± 3.46	51.83 ± 1.35	<u>61.23 ± 2.71</u>	48.34 ± 0.76	50.51 ± 1.05	50.04 ± 0.86	N/A	56.73 ± 0.69	62.32 ± 1.02
Contact	95.37 ± 0.92	91.89 ± 0.38	96.53 ± 0.10	94.84 ± 0.75	89.07 ± 0.34	93.05 ± 0.09	92.83 ± 0.05	N/A	<u>98.30 ± 0.02</u>	98.36 ± 0.02	
Avg. Rank	5.67	6.83	6.25	4.25	5.17	6.92	6.08	N/A	<u>2.42</u>	1.42	
hist	Wikipedia	61.86 ± 0.53	57.54 ± 1.09	78.38 ± 0.20	75.75 ± 0.29	62.04 ± 0.65	79.79 ± 0.96	82.87 ± 0.21	<u>82.08 ± 0.32</u>	68.33 ± 2.82	75.97 ± 0.75
	Reddit	61.69 ± 0.39	60.45 ± 0.37	64.43 ± 0.27	64.55 ± 0.50	64.94 ± 0.21	61.43 ± 0.26	64.27 ± 0.13	<u>66.79 ± 0.31</u>	64.81 ± 0.25	66.80 ± 0.35
	MOOC	64.48 ± 1.64	64.23 ± 1.29	74.08 ± 0.27	77.69 ± 3.55	71.68 ± 0.94	69.82 ± 0.32	72.53 ± 0.84	<u>81.52 ± 0.37</u>	80.77 ± 0.63	82.74 ± 0.75
	LastFM	68.44 ± 3.26	68.79 ± 1.08	69.89 ± 0.28	66.99 ± 5.62	67.69 ± 0.24	55.88 ± 1.85	70.07 ± 0.20	<u>72.63 ± 0.16</u>	70.73 ± 0.37	72.79 ± 0.30
	Enron	65.32 ± 3.57	61.50 ± 2.50	57.84 ± 2.18	62.68 ± 1.09	62.25 ± 0.40	64.06 ± 1.02	68.20 ± 1.62	70.09 ± 0.65	65.78 ± 0.42	<u>68.33 ± 1.54</u>
	Social Evo.	88.53 ± 0.55	87.93 ± 1.05	91.87 ± 0.72	92.10 ± 1.22	83.54 ± 0.24	93.28 ± 0.60	93.62 ± 0.35	<u>96.94 ± 0.17</u>	96.91 ± 0.09	96.99 ± 0.11
	UCI	60.24 ± 1.94	51.25 ± 2.37	62.32 ± 1.18	62.69 ± 0.90	56.39 ± 0.10	70.46 ± 1.94	<u>75.98 ± 0.84</u>	76.01 ± 0.75	65.55 ± 1.01	73.94 ± 0.99
	Can. Parl.	51.62 ± 1.00	52.38 ± 0.46	58.30 ± 0.61	55.64 ± 0.54	60.11 ± 0.48	57.30 ± 1.03	56.68 ± 1.20	N/A	<u>88.68 ± 0.74</u>	89.27 ± 0.63
	US Legis.	58.12 ± 2.94	67.94 ± 0.98	49.99 ± 4.88	<u>64.87 ± 1.65</u>	54.41 ± 1.31	52.12 ± 2.13	49.28 ± 0.86	N/A	56.57 ± 3.22	64.97 ± 2.23
	UN Trade	58.73 ± 1.19	57.90 ± 1.33	59.74 ± 0.59	55.61 ± 3.54	<u>60.95 ± 0.80</u>	61.12 ± 0.97	59.88 ± 1.17	N/A	58.46 ± 1.65	60.34 ± 0.17
	UN Vote	<u>65.16 ± 1.28</u>	63.98 ± 2.12	51.73 ± 4.12	68.59 ± 3.11	48.01 ± 1.77	54.66 ± 2.11	45.49 ± 0.42	N/A	53.85 ± 2.02	61.54 ± 0.54
Contact	90.80 ± 1.18	88.88 ± 0.68	93.76 ± 0.41	88.84 ± 1.39	74.79 ± 0.37	90.37 ± 0.16	90.04 ± 0.29	N/A	<u>94.14 ± 0.26</u>	94.28 ± 0.08	
Avg. Rank	6.00	7.00	5.33	5.33	6.17	5.08	4.58	N/A	<u>3.67</u>	1.83	
ind	Wikipedia	61.87 ± 0.53	57.54 ± 1.09	78.38 ± 0.20	75.76 ± 0.29	62.02 ± 0.65	79.79 ± 0.96	<u>82.88 ± 0.21</u>	83.17 ± 0.31	68.33 ± 2.82	75.94 ± 0.75
	Reddit	61.69 ± 0.39	60.44 ± 0.37	64.39 ± 0.27	64.55 ± 0.50	<u>64.91 ± 0.21</u>	61.36 ± 0.26	64.27 ± 0.13	64.51 ± 0.19	64.80 ± 0.25	66.78 ± 0.36
	MOOC	64.48 ± 1.64	64.22 ± 1.29	74.07 ± 0.27	77.68 ± 3.55	71.69 ± 0.94	69.83 ± 0.32	72.52 ± 0.84	75.81 ± 0.69	<u>80.77 ± 0.63</u>	82.75 ± 0.75
	LastFM	68.44 ± 3.26	68.79 ± 1.08	69.89 ± 0.28	66.99 ± 5.61	67.68 ± 0.24	55.88 ± 1.85	70.07 ± 0.20	<u>71.42 ± 0.33</u>	70.73 ± 0.37	72.79 ± 0.30
	Enron	65.32 ± 3.57	61.50 ± 2.50	57.83 ± 2.18	62.68 ± 1.09	62.27 ± 0.40	64.05 ± 1.02	68.19 ± 1.63	68.79 ± 0.91	65.79 ± 0.42	<u>68.33 ± 1.54</u>
	Social Evo.	88.53 ± 0.55	87.93 ± 1.05	91.88 ± 0.72	92.10 ± 1.22	83.54 ± 0.24	93.28 ± 0.60	93.62 ± 0.35	96.79 ± 0.17	<u>96.91 ± 0.09</u>	96.99 ± 0.11
	UCI	60.27 ± 1.94	51.26 ± 2.40	62.29 ± 1.17	62.66 ± 0.91	56.39 ± 0.11	70.42 ± 1.93	75.97 ± 0.85	73.41 ± 0.88	65.58 ± 1.00	<u>73.91 ± 0.99</u>
	Can. Parl.	51.61 ± 0.98	52.35 ± 0.52	58.15 ± 0.62	55.43 ± 0.42	60.01 ± 0.47	56.88 ± 0.93	56.63 ± 1.09	N/A	<u>88.51 ± 0.73</u>	88.65 ± 0.94
	US Legis.	58.12 ± 2.94	67.94 ± 0.98	49.99 ± 4.88	64.87 ± 1.65	54.41 ± 1.31	52.12 ± 2.13	49.28 ± 0.86	N/A	56.57 ± 3.22	<u>64.97 ± 2.23</u>
	UN Trade	58.71 ± 1.20	57.87 ± 1.36	59.98 ± 0.59	55.62 ± 3.59	<u>60.88 ± 0.79</u>	61.01 ± 0.93	59.71 ± 1.17	N/A	57.28 ± 3.06	60.29 ± 0.16
	UN Vote	<u>65.29 ± 1.30</u>	64.10 ± 2.10	51.78 ± 4.14	68.58 ± 3.08	48.04 ± 1.76	54.65 ± 2.20	45.57 ± 0.41	N/A	53.87 ± 2.01	61.52 ± 0.58
Contact	90.80 ± 1.18	88.87 ± 0.67	93.76 ± 0.40	88.85 ± 1.39	74.79 ± 0.38	90.37 ± 0.16	90.04 ± 0.29	N/A	<u>94.14 ± 0.26</u>	94.28 ± 0.08	
Avg. Rank	6.00	6.92	5.25	5.33	6.17	5.08	4.67	N/A	<u>3.75</u>	1.83	